UNIVERSITÀ
degli STUDI
di CATANIA

DEPARTMENT OF CLINICAL AND EXPERIMENTAL MEDICINE

PhD in 'Translational Biomedicine'

XXXIV cycle

Studies of a restricted signature of circulating miRNAs as non-invasive biomarker in glioma: from the molecular function to the clinical application

Ana Belén Díaz Méndez

Coordinator: **Prof. Lorenzo Malatino**

Internal Supervisor: **Prof. Michele Purrello**

External Supervisor: **Dr. Maria Giulia Rizzo**

INDEX

ABSTRACT

Gliomas are diffusely growing brain tumours and challenging cancers for diagnosis and treatment. The identification of genetic and epigenetic markers has led to an integrated diagnosis, composed of a histological diagnosis, and a molecular profile of the tumour. Among the key genetic events, mutations of the isocitrate dehydrogenase (IDH) genes are noteworthy. Altered miRNA profiles have been observed not only in tumour tissues but also in biofluids, where they circulate in a very stable form, making them interesting candidate as biomarkers. Several circulating miRNAs have been evaluated in gliomas as single biomarkers. However, it is widely recognized that single miRNA profiles may provide a low accuracy as cancer biomarkers, mostly due to the multifactorial nature of tumour and to the large number of targets for a single miRNA.

In this thesis work we identified a ten-serum miRNA signature dysregulated between IDH wild-type and IDH mutant patients that shows diagnostic and prognostic value. Interestingly, among them, the combination of miR-1-3p, miR-26a-1-3p and miR-487b-3p led to an improvement of the diagnostic performance, compared to each single miRNA of the signature, and also allows to discriminate glioma patients from healthy subjects. We also found that alteration of miR-1-3p, miR-26a-1-3p and miR-487b-3p in serum may reflect their changes in tumour tissue, and cell lines recapitulate what observed in glioma patients. Moreover, we showed that the combination of miR-1/-26a-1/-487b acts as tumour suppressor in IDH-wt glioma cells by exerting an increased adverse effect on cell viability, proliferation and migration, and inducing apoptosis and cell cycle arrest. Finally, we identified predicted important targets of the restricted miRNA signature which are part of potential targetable enriched pathways. Altogether these results suggest that a restricted miRNA signature could provide a complementary approach, using circulating miRNAs from blood, to help patients diagnosis and monitoring of brain tumour growth.

INTRODUCTION

Brain tumours

Brain tumours are malignancies that develop within the central nervous system (CNS), they rank 18th among the most common tumours in the world (Figure 1). In the paediatric field, they represent the most frequent type of solid cancer (epidemiological data from the International Agency for Research on Cancer - IARC).

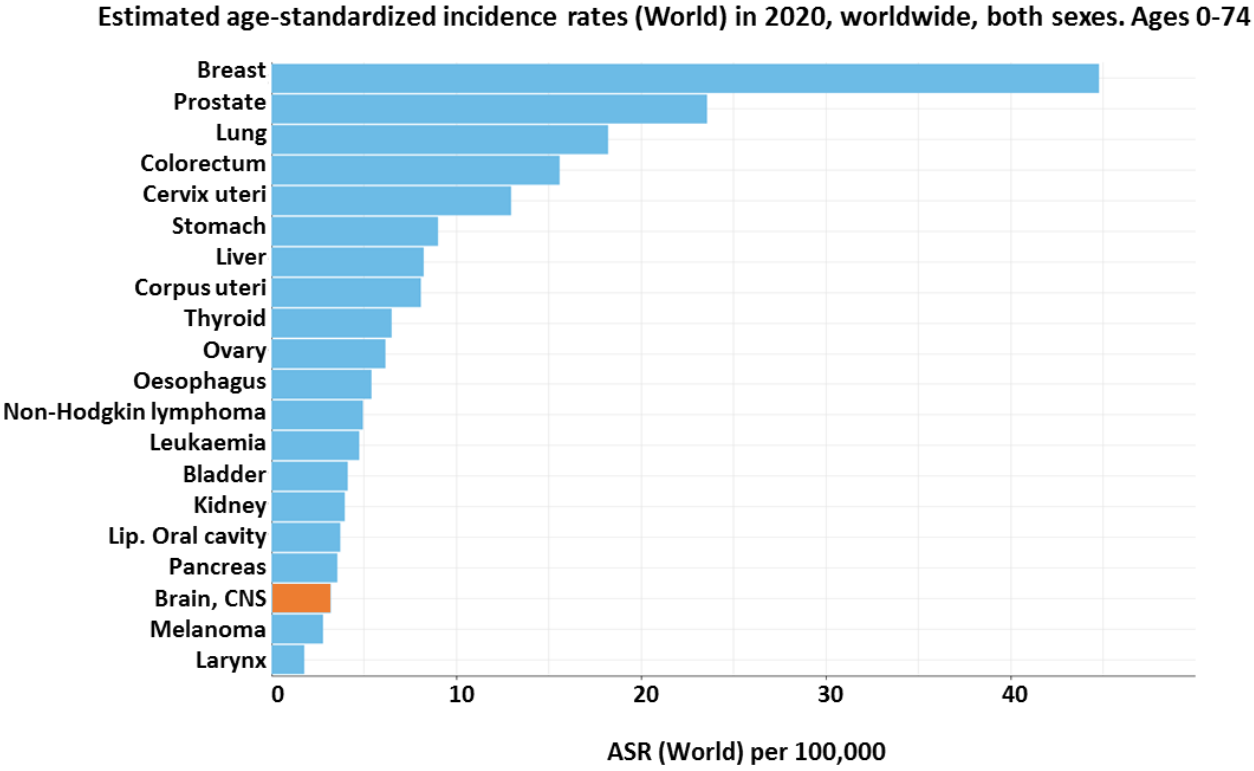

Figure 1: Incidence rate of the 20 most common cancers worldwide. The graph shows the incidence in the world of the indicated tumours, the values are standardized according to age (age standardized rate, ASR) and expressed per 100000, refer to both sexes and all age groups, according to data obtained by the online platform " Global Cancer Observatory" established by the IARC agency (https://gco.iarc.fr/), the bar highlighted in orange indicates brain tumours.

The first basic distinction between the different types of malignancies that can affect the nervous system is based on the tumour origin and allows to discriminate between primary, or primitive, brain tumours that develop directly in the tissues of the central nervous system, and secondary-derived tumours, or brain metastases that originate from malignancies whose primary location is found in other parts of the body. This second group is the most common intracranial tumour form, and in fact, it is believed that the incidence of brain metastases is up to 10 times higher than

primitive brain tumours (*McFaline-Figueroa JR et al., 2018; Arvold ND et al., 2016*). Although several solid tumours can metastasize to the brain, the most frequent types of brain metastases come from lung, breast, and melanoma cancers (*Nayak L et al., 2012*).

Primary brain tumours represent a heterogeneous group of malignancies that develop from cells and tissues inside the central nervous system, being meningiomas and gliomas the most representative types of primitive intracranial cancers (*McFaline-Figueroa JR et al., 2018*).

- **Gliomas**

Gliomas account for 75% of primitive malignant brain tumours in adults. They are tumours of neuroectodermal origin that derive from glial cells or precursors and can be divided according to the cell type from which they originate into astrocytoma, oligodendroglioma and ependymoma (*Lapointe S et al., 2018*). Glioma comprises a large group of heterogeneous malignancies with variable clinical frameworks, ranging from low-grade, circumscribed and slow-growing tumours to high-grade, infiltrating tumours characterised by cancer cells that invade the surrounding cerebral parenchyma, which are virtually incurable (*Pisapia DJ et al., 2017; Altwairgi AK et al., 2017; Louis DN et al., 2020*).

- **Diagnosis of Glioma and WHO 2016 Classification**

One of the peculiar characteristics of gliomas, especially the infiltrating ones, is that, unlike for other solid tumours, no pre-neoplastic lesions have ever been described that precede the development of this type of neoplasm without presenting invasive features and with the possibility of being surgically removed. Therefore, by the time the tumour mass is detected, the disease is already in progression and invading the surrounding tissues (*Pisapia DJ et al., 2017*).

Gliomas spread almost exclusively within the nervous system while the formation of metastases in other organs is extremely rare, consequently imaging techniques, such as magnetic resonance imaging (MRI), at the brain level are the main methods through which the initial detection of these tumours is carried out (*Reni M et al., 2017*) and the disease is monitored during its clinical course (*Visser M et al., 2019*). MRI allows to visualize changes in blood oxygenation levels induced by a modulation of brain activity, this method is used to assess the possibility of surgical removal of the tumour, particularly when located near eloquent areas such as the motor cortex or areas of language (*Reni M et al., 2017*).

Histological analysis of neoplastic tissue, taken by biopsy or as a result of surgical removal of the tumour mass, is of fundamental importance to define the diagnosis, determine the degree of the tumour and the most appropriate type of therapy (*Altwairgi AK et al., 2017; Reni M et al., 2017*). Until five years ago, gliomas were classified, according to the World Health Organization (WHO) indications, into four different tumour grades based on immunohistochemical characteristics of the cancer tissue: grade I glioma, mostly circumscribed and non-invasive, grade II and III glioma more widespread and infiltrating behaviour and grade IV gliomas, or glioblastomas (GBMs), which constitute the most aggressive and malignant type (*Louis DN et al., 2007*). The discovery of significant driver mutations such as those in the isocitrate dehydrogenase (*IDH*), *BRAF*, or histone genes has fundamentally changed the diagnostic approach in neuropathology (*Capper D et al., 2010; Khuong-Quang DA et al., 2012*). This biomarker-driven classification is reflected in the 2016 update of the WHO classification of CNS tumours (Figure 2). This has resulted in the concept of an integrated diagnosis, composed of a histological diagnosis and a molecular profile. (*Shaikh N et al., 2018; Barnholtz-Sloan JS et al., 2018*).

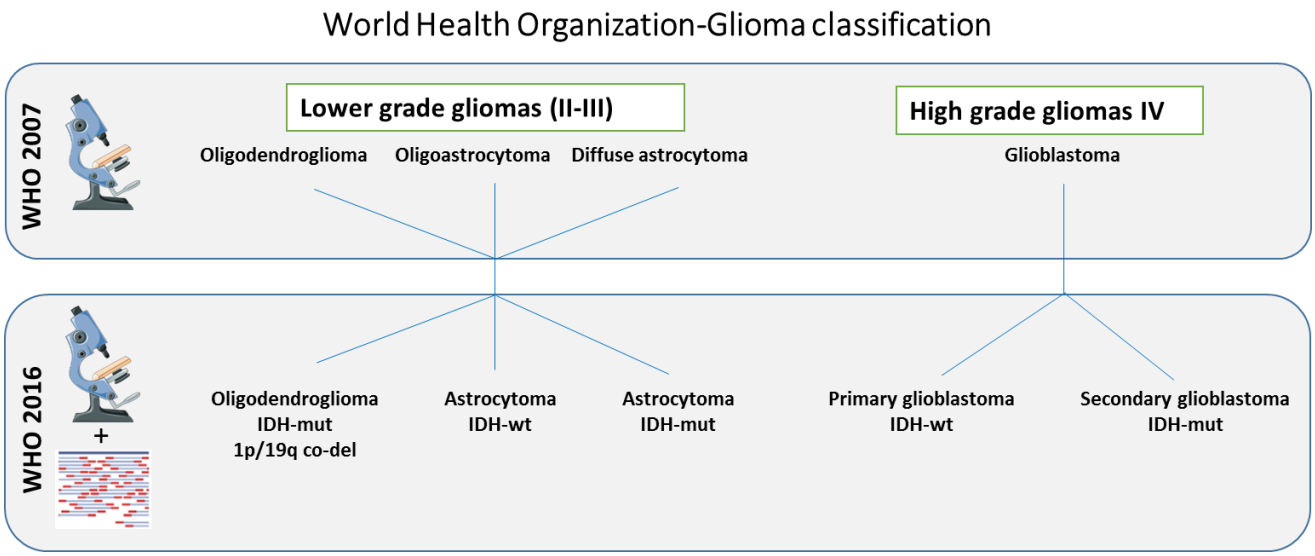

Figure 2: The 2007 WHO classification of brain tumours and 2016 update. Comparison between the subtypes of grade II-IV gliomas based on the 2007 WHO classification and the new categories established by the 2016 revision. 1p/19q co-del=codelection of chromosome portions 1p and 19q; IDH-wt= IDH wild type gene; IDH-mut= IDH mutated gene. (Figure modified from *Louis N D et al., 2016*).

After histological examination, the diagnostic approach is followed by immunohistochemistry and subsequent genetic or epigenetic analysis to determine mutations defining a tumour type or even to establish a methylation class (*Louis DN et al., 2020; Capper D et al., 2018*). This diagnostic

workup requires tumour material, i.e. a brain biopsy which can be limited (for example stereotactic) but can also be an extensive debulking.

- **IDH genes in gliomas**

Among the driver mutations, those occurring in the IDH genes are particularly important form a clinical point of view for their diagnostic and prognostic implications (*Han S et al., 2020*). Isocitrate dehydrogenases are enzymes that catalyse the decarboxylation of the isocitrate into ketoglutarate with concomitant reduction of the nicotine cobalt adenine dinucleotide phosphate (NADP) in NADPH. Under physiological conditions, a balance is established between isocitrate and ketoglutarate, reflecting the energy state of the cells. In glial cells, IDH enzymes also regulate glutamine and glutamate metabolism. In hypoxic conditions cells focus the synthesis of lipids almost exclusively on the transformation of the ketoglutarate resulting from the metabolism of glutamine, this metabolic shift from glucose consumption through the Krebs cycle to glutamine reduction is a frequent characteristic observed in gliomas (*Turkalp Z et al., 2014; Metallo CM et al., 2012*). In addition, IDH enzymes play an important role in the cell response to oxidative stress conditions, since NADPH production is important for glutathione regeneration which plays a fundamental role as an endogenous antioxidant, particularly in brain tissues where the reactions catalysed by IDH enzymes are the main sources of NADPH in the cell (*Romanidou O et al., 2018*). There are three isoforms of IDH encoded by the genes *IDH1, IDH2* and *IDH3*. The IDH1 enzyme derived performs its function in the cytosol and peroxisomes, while the other two isoforms are mitochondrial enzymes. Through genome sequencing techniques, Parson and colleagues first identified the presence of *IDH1* mutations in a small category of GBM patients in 2008 (*Parsons DW et al., 2008*). This observation was later supported by studies in The Cancer Genome Atlas (TCGA) project (*Turkalp Z et al., 2014*). Mutations in *IDH1* and, less frequent *IDH2* genes are observed in the majority of grade II or III gliomas, with a frequency of about 90% for oligodendrogliomas and 70 % for astrocytomas. In contrast, this type of mutations is rarely observed in glioblastomas. The majority of GBM patients normally retain the wild-type form of *IDH* genes, just a very small portion harbour mutations in these genes and they are usually suffering from secondary glioblastomas that progress from lower-grade gliomas (*Turkalp Z et al., 2014*). The presence of mutations in *IDH* genes is therefore considered an important molecular marker as it identifies a subcategory of glioma showing less aggressive characteristics, a better prognosis and a greater response to chemotherapy treatments (*Turkalp Z et al., 2014; Metallo CM*

et al., 2012). Mutations in *IDH1* and *IDH2* genes are events that occur very early during glioma tumorigenesis, constituting initiating mutations. They invariably appear in heterozygotic form as missense mutations that lead to the modification of a single amino acid residue (*Romanidou O et al., 2018*). The most frequent alterations occur at the *IDH1* gene, at the level of codon 132 and lead to the replacement of an arginine that is located at the active site of the enzyme and is involved in the link with the substrate. In the 90% of cases, it is replaced with a histidine residue (R132H mutation), however, other types of less frequent amino acid substitutions have also been observed in the codon level 132 of this gene (R132S, R132G, R132C, R132L). A portion of patients who retain the wild-type *IDH1* gene, on the other hand, shows mutations at the codon 172 level of the *IDH2* gene, which also encodes for an arginine residue (*Romanidou O et al., 2018; Deng L et al., 2018*). The mutated forms of *IDH* both have a loss of their physiological function since these enzymes show a decreased affinity for the isocitrate and an increase in affinity for NADPH, and at the same time a gain of function due to the ability to catalyse the transformation of the ketoglutarate into 2-dyhydroxyglutarate (D-2HG) with a concomitant oxidation of NADPH (Figure 3; *Chen R et al., 2017; Mondesir J et al., 2016*).

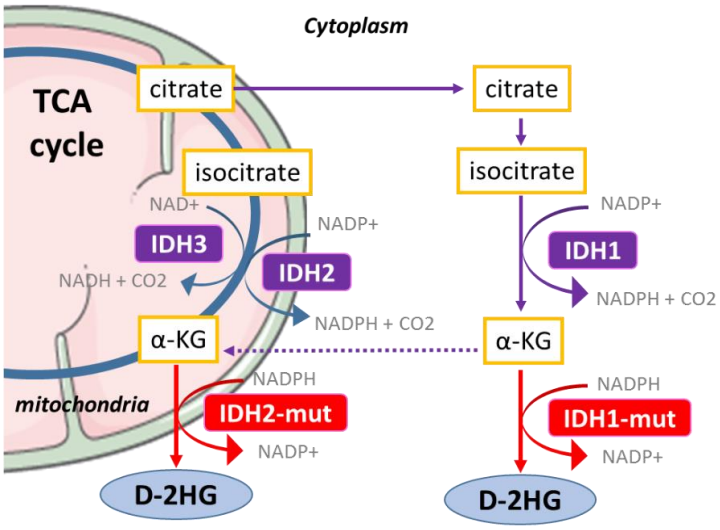

Figure 3. Enzymatic activities of IDH- wild type and IDH-Mutant (Figure adapted from *Mondesir J et al., 2016*)**.**

D-2HG acts as oncometabolite due to its inhibitory action on key enzymes for the regulation of histones and DNA methylation. Thus, the presence of *IDH* mutations is accompanied by a general alteration of chromatin methylation levels with a far-reaching impact on the regulation of gene expression. *IDH* mutations are frequently associated with a condition of CpG island

hypermethylation in gliomas, while this phenotype is not found in *IDH* wild-type gliomas (*Turkalp Z et al., 2014*). The Glioma CpG island methylator phenotype (G-CIMP) observed in patients with *IDH1/2* mutations may explain the association of these alterations with a better prognosis and an increased response to therapy: one of the key genes whose promoter is hypermethylated in these gliomas is in fact, the one that encodes for *O6-methylguanine-DNA methyltransferase (MGMT)* (*Bady P et al., 2012*), another fundamental prognostic and predictive molecular marker used to guide the choice of therapy for these patients. *MGMT* is a DNA repair protein, which removes the cytotoxic O6-methylguanine DNA lesions generated by temozolomide (TMZ), the standard chemotherapy for newly diagnosed glioma (*Chen X et al., 2018*).

MicroRNA

In recent years, the advent of new high-throughput technologies, such as Next Generation Sequencing (NGS), has revealed that most of the eukaryotic genome is subject to transcription, only the 1-2% of transcripts are then translated into proteins and the remaining part constitutes a broad category of non-coding RNA molecules (*non-coding RNA*, ncRNA), in turn divided into numerous classes of molecules with specific characteristics (Figure 4). Since many ncRNAs show an expression profile that follows defined spatio-temporal patterns and often present specific sub-cellular localization, this suggests that these transcripts play precise functional roles within the cell (*Da Sacco L et al., 2012*).

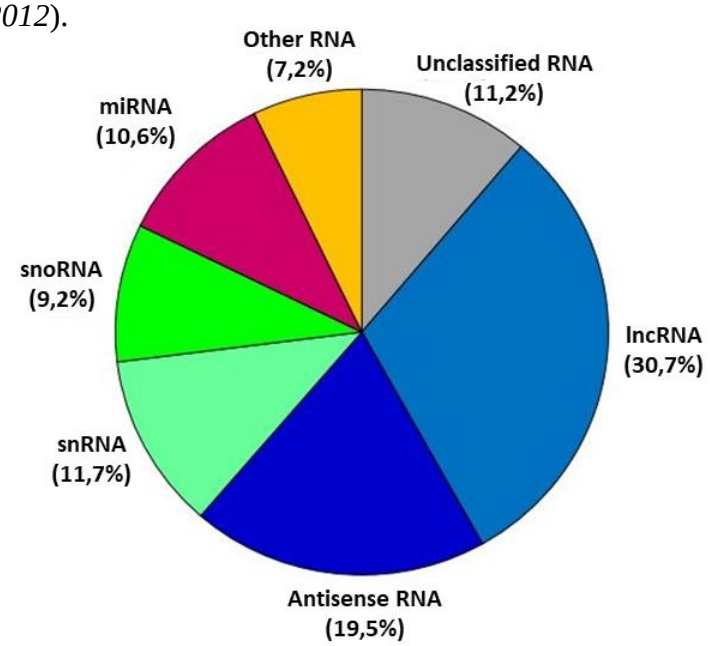

Figure 4: Classification of non-coding RNAs. The graph shows the main classes of ncRNA and the respective percentages of distribution in the human genome. miRNA=microRNA; lncRNA = long non-coding RNA; snRNA= small nuclear RNA; snoRNA = small nucleolar RNA (Figure modified from *Da Sacco L et al., 2012*).

One of the most studied classes of ncRNA are microRNAs (miRNAs), small non-coding RNAs, with a sequence of about 18-24 nucleotides, which play an important and broad role in the regulation of gene expression through post-transcriptional mechanisms that influence the translation of messenger RNA (mRNA) into proteins (*Acunzo M et al., 2015*). The discovery of their existence dates back to about 25 years ago and derives from a research, carried out at Robert Horviz's laboratory, aimed at defining the neural development of the nematode *Caenorhabditis elegans* in heterochronic mutants that present alterations in the correct temporal development of the embryo (*Horvitz H.R et al., 1980)*. Concretely, mutations were identified in two gene loci, *lin-4* and *lin-14*, which presented opposite alterations in larval development and the phenotype due to the mutation of *lin-4* is reversed by the loss of function of *lin-14* (*Orellana EA et al., 2015*). These observations therefore led the researchers to hypothesize that the product of the *lin-4* gene had an inhibitory action on *lin-14*, however two studies published in 1993 showed that the *lin-4* gene did not code for any protein product but for two short RNAs long 22 and 61 nucleotides respectively *(Lee RC et al, Cell, 1993*). The presence of seven elements in the 3'untranslated region (3'UTR) of the *lin-14* mRNA was also identified with a complementary sequence to that of the small RNA encoded by *lin-4* (*Wightman B et al., 1993*). These studies led to the identification of a mechanism by which a gene encoding a small RNA, a microRNA, was able to repress the expression of a second gene by pairing with related mRNA. A few years later, other genes encoding for miRNAs were identified with homologs in numerous plant and animal species, including humans (*Orellana EA et al., 2015; Lagos-Quintana M et al., 2001*; *Reinhart BJ et al., 2002*), demonstrating that miRNAs are conserved through evolution and constitute a mechanism of gene regulation shared by all eukaryotes (*Orellana EA et al., 2015*).

In 2002 miRBase was created, the first *online* database that collects the sequences of all potential miRNAs identified in the different species, in the current version 2654 mature miRNA sequences and 1917 precursor sequences for humans are collected (http:/www.mirbase.org/cgi-bin/browse.pl?org=hsa). In Figure 5, selected hallmarks of microRNAs history are illustrated (*Thomas KT et al., 2018*).

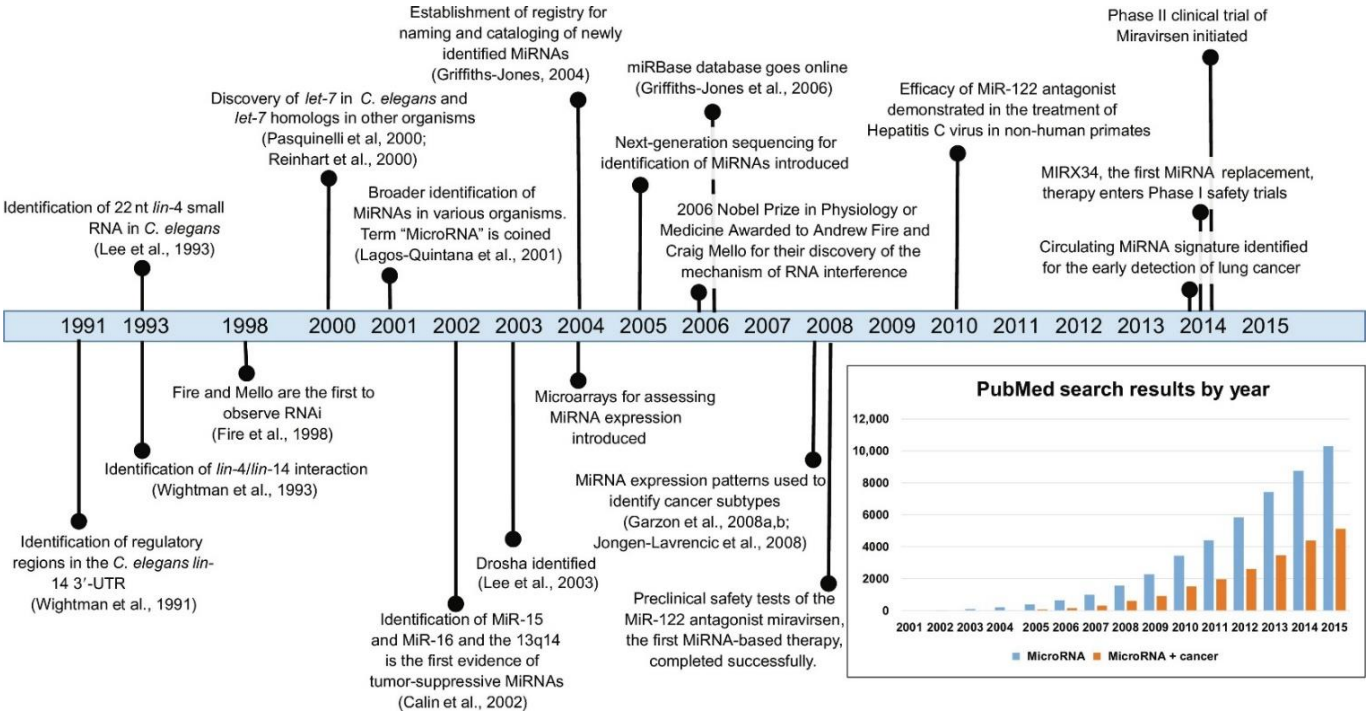

Figure 5: The timeline noticeable key discoveries in the history of miRNA research. (Figure taken from *Thomas KT et al., 2018*).

- **MicroRNA Biogenesis and function**

Based on the localization in the genome and the organization of the genes that code for miRNAs, these small RNAs can be classified into intronic miRNAs, located in introns of genes that code for other longer transcripts, exonic miRNAs, located in exons of genes that do not code for proteins, monocistronic or polycistronic miRNAs, depending on whether the RNA produced by the transcription contains a single microRNA or an entire cluster of miRNAs (*Liu X et al., 2008*). It is thought that about 50% of miRNAs are expressed through transcripts that do not encode for proteins, the rest is mainly located in introns of coding genes and their expression is therefore linked to that of the host gene although they are subsequently processed separately to give rise to mature miRNA (*Bhaskaran M et Al., 2014*).

MiRNAs derive from precursor RNAs through a sequential and compartmentalized maturation process: the genes encoding miRNAs are transcribed as precursors in the nucleus by the RNA polymerase II and give rise to primary transcripts, pri-miRNA, which undergo end capping 5 'and polyadenylation (*Bhaskaran M et al., 2014*). These molecules fold to form a hairpin structure (*stem-loop*) with a double-stranded region about 33 base pairs long, a loop at one end and two unpaired single-stranded regions at the other end. This structure is recognized and bound by an

RNA binding protein, DGCR8/Pasha, which recruits a type III RNase, Drosha, which catalyses a staggered cleavage at the level of the double-stranded region. In this way, an intermediate precursor is produced, defined pre-miRNA, about 70-100 nucleotides long which retains a *stem-loop* structure with a 5 'phosphate end and two protruding nucleotides at the 3' end (*Liu X et al., 2008*). The pre-miRNA is then exported to the cytoplasm via the nucleus-cytoplasmic transporter complex Esportin 5/RanGTP. The maturation process continues in the cytoplasm through the action of the Dicer/TRBP complex. Dicer is also a type III RNase containing a PAZ domain that recognizes and binds the protruding 3 'end of the pre-miRNA, the ribonuclease domain therefore cuts the *stem-loop* structure producing a double-stranded RNA about 20 base pairs long with staggered ends (*Liu X et al., 2008; Zhang H et al., 2004*). The two strands of the duplex RNA are then separated, one of them, called the "*guide*" strand, gives rise to the mature miRNA while the other strand, called "*passenger*", usually undergoes degradation, although in some cases both strands give rise to miRNAs with regulatory functions within the cell. The guide filament is incorporated into a ribonucleoprotein RNA-induced silencer complex (RISC), that contains the AGO2 protein belonging to the Argonaute family of proteins with nuclease activity (Figure 6, *Liu et al., 2008*). The guide strand contains a short sequence of about 8 nucleotides defined seed sequence on the basis of which the RISC complex is directed towards the target mRNA which has, generally within the 3'UTR region, a complementary sequence (*Romero-Cordoba SL et al., 2014*). The binding with the RISC complex determines the degradation of the mRNA or the inhibition of its translation and sequestration within cellular structures called P bodies. It is believed that the choice of one mechanism of action over the other depends on the level of complementarity between the miRNA and its target: a complete pairing induces the degradation of the mRNA while a partial complementarity determines the inhibition of translation (*Eulalio A et al., 2007; Eulalio A et al., 2008*).

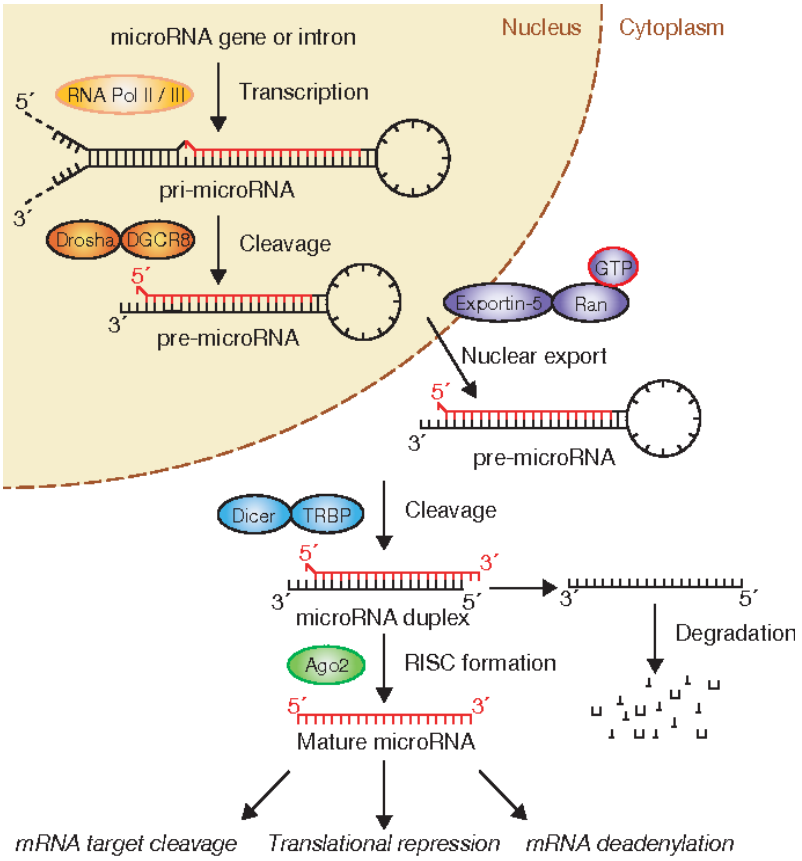

Figure 6: Overview of miRNA processing. Schematic representation of the maturation processes of the microRNAs (Figure taken from *Liu et al., 2008*).

Bioinformatics analyses and transcriptomics and proteomics studies have revealed how each miRNA can potentially regulate the expression of hundreds of target genes. In fact, the involvement of these small non-coding RNAs in almost every biological process studied up to now has been demonstrated, however miRNAs, rather than showing a dramatic impact on the expression of their targets, act more as modulators of gene expression (*Coolen M et al., 2009*). Numerous studies have shown that microRNAs play an important role in the regulation of dynamic processes such as embryonic development, cell proliferation and differentiation. Consequently, it has been observed that an aberrant miRNA expression is linked to the development of numerous types of pathologies (*Vreugdenhil E et al., 2010*). In the brain, more than in other organs, the expression of a wide variety of miRNAs has been observed, furthermore a large number of them are enriched or specifically expressed in the brain, this probably reflects the complexity and variety of cell types which make up the central nervous system (*Vreugdenhil E et al., 2010*). It has been observed that brain development processes are accompanied by a dynamic and temporally defined regulation of the miRNA expression, so that specific sets of miRNAs are expressed at certain stages of the embryonic development of the nervous system (*Vreugdenhil E et al., 2010*).

- **MicroRNAs in Cancer and Glioma**

The first evidence concerning the involvement of miRNAs in tumour development dates back to the studies carried out by Croce and colleagues on the miR-15a-16-1 cluster which is frequently deleted in cases of chronic lymphocytic leukaemia (*Calin GA et al., 2002*). The number of researches that relate miRNAs to tumour pathogenesis has increased exponentially, revealing that the vast majority of tumours present characteristic miRNA expression profiles, different from the non-tumour counterpart of the same tissues and organs (*Di Leva G et al., 2014*). Also, in many cases, these alterations in the expression of microRNAs are correlated to the clinical-pathological characteristics of the tumour examined, such as the grade, stage, proliferation index, vascularization, etc. Since miRNAs can potentially regulate hundreds of target transcripts expressed in different types of cells and tissues, some of them can play different roles depending on the tumour type, acting alternatively as promoters (oncomiR) or tumour suppressors (*Di Leva G et al., 2014; Coolen M et al., 2009*). Also in gliomas, as in many other types of cancer, microRNAs play an important role in the processes that lead to the formation and progression of the tumour. In the last decade, numerous studies of molecular biology and gene expression have been carried out that have led to the identification of microRNA expression profiles characteristic of glioma tumour cells (*Ahir BK et al., 2017*). Identifying the function of these miRNAs in glioma biology can help to establish their potential use as biomarkers or as therapeutic targets for these tumours (*Ahir BK et al., 2017*). MiR-21 is one of the first miRNAs discovered in relation to gliomas. Many studies have demonstrated its increased expression in this type of tumour compared to normal brain tissues (*Belter et al., 2016*). MiR-21 promotes the invasiveness of glioma cells because among its targets there are several inhibitors of matrix metalloproteinases, proteolytic enzymes that degrade the extracellular matrix favouring invasive processes. The inhibition of miR-21 causes a reduction in invasiveness both in cell lines and in xenograft models of glioma (*Wang S et al., 2018; Beyer S et al., 2017*). Some miRNAs influence the behaviour of cancer cells by modulating signalling pathways that regulate cell survival or proliferation. One example is miR-7 which acts as a tumour suppressor in gliomas since it directly inhibits both *EGFR* (a frequently overexpressed and hyperactive receptor in gliomas) and other components of the downstream signalling pathway, such as the kinases *PI3K* and *Raf-1* (*Shea A et al., 2016*; *Liu Z et al., 2014*). Transfection of this miRNA into GBM cell lines induces apoptosis and decreases invasiveness by inhibiting the focal adhesion kinase (*FAK*) (*Shea A et al., 2016*; *Ahir BK et al., 2017*). MiR-7 also

acts as a regulator of angiogenesis since it represses the expression of the VEGF receptor, VEGFR2 (*Shea A et al., 2016*) through indirect mechanisms. Another miRNA implicated in angiogenesis mechanisms is miR-210 which targets HIF3A, a protein inhibiting the response to hypoxia that negatively regulates the production of VEGF (*Shea A et al., 2016; Banelli B et al., 2017; Rooj AK et al., 2016*). The expression of miR-210 in gliomas increases under hypoxic conditions. In these circumstances it can also be secreted by tumour cells inside extracellular vesicles and affect the endothelial cells of the blood vessels adjacent to the tumour (*Rooj AK et al., 2016*). In the lab where this thesis was performed, it was investigated a restricted signature of circulating/serum miRNAs, including miR-15b, -23a, −99a, −125b, −133a, −150, −197, −340, −497, −548b and let-7c, as potential non-invasive biomarker in the diagnosis of glioma patients. Among them, serum miR-497 and -125b expression levels were decreased in higher glioma grades and show high sensitivity and specificity in discriminating patients with GBM from lower grade gliomas (*Regazzo et al., 2016*). Lastly, the alteration of microRNA expression profiles in gliomas is often linked to epigenetic mechanisms. In fact, there are numerous cases of miRNA whose genes have altered levels of methylation in the promoter region, one example being the miR-204 and miR-145, both implicated in the regulation of the stem-like phenotype of cancer cells, having *SOX4* genes as targets and *SOX2*, respectively (*Banelli B et al., 2017*).

Liquid biopsy

The current gold standard of cancer diagnosis is the histological examination of tumour tissue, obtained either by radiologically guided biopsy or surgical excision. However, these procedures are invasive, expensive, and risky for the patient. Moreover, the molecular profile of the tumour evolves dynamically over time in response to a wide variety of endogenous and exogenous selective pressures, for instance distinct metastatic lesions that can be molecularly divergent from the primary tumour, or the therapeutic stress can dynamically modify the genomic landscape of tumour. Tissue biopsies have a limited capability of capturing these dynamic changes in the tumour. Therefore, there is a clinical need for alternative diagnostic techniques. In particular, the use of biological fluids such as blood as a source of non-invasive cancer biomarkers has raised a great deal of interest. So-called “liquid biopsies” hold great clinical promise, as their non-invasive nature allows for rapid, economical, and repeat sampling-features that permit their use for the monitoring of treatment response and disease progression (*Larrea E et al., 2016*; *Siravegna G et al., 2019*). Liquid biopsy is based on the fact that tumours can shed their molecular content such

as proteins or cell-free nucleic acids (cfNAs), into body fluids, either as cell-free entities, attached to lipid or protein structures or as the content of extracellular vesicles, such as exosomes. Several classes of cfNAs are detected: DNA and different classes of RNA such as protein-coding mRNA and non-coding RNAs, including miRNAs and long-non coding RNAs (lncRNAs) (*Diaz Mendez AB et al., 2021*).The diagnostic workup in glioma requires the analysis of tumour material, obtained by a brain biopsy which can pose a risk for patients not amenable of surgical intervention. After surgery, disease is monitored by MRI. However, in patients with adjuvant radio- and chemotherapy it may be difficult, by imaging techniques, to reliably discriminate tumour progression from radiation necrosis (*Müller Bark J et al., 2020*). To overcome these barriers, liquid biopsies has been proposed as a potential tool for prognosis and diagnosis determination in glioma (*Panditharatna E et al., 2018; Müller Bark J et al., 2020*). The presence of the blood-brain barrier (BBB) must be considered when dealing with applicability of circulating biomarkers in glioma management. BBB is a structure that establishes a diffusion barrier between the blood circulation and the CNS, essential for the maintaining of homeostasis of the brain microenvironment and for the normal functioning of the brain (*Wolburg H et al., 2012; Ballabh P et al., 2004*). An essential role for BBB function is played by the tight junctions that connect BBB endothelial cells: unlike other blood vessels endothelial cells, they lack fenestrations, are characterized by a very reduced perivascular space and have more extensive tight junctions that limit the paracellular flux of hydrophilic molecules across the BBB. Small hydrophobic compounds can diffuse across BBB crossing plasma membranes while passage of nutrients or large molecules is actively regulated by transporters or receptor-mediated endocytosis (*Ballabh P et al., 2004).* The BBB integrity is often compromised in gliomas with different degrees of disruption in different stages and grades, or instance a loss of claudin-3 from the BBB has been reported in GBM (*Wolburg H et al., 2003*). These changes in BBB permeability can be observed by MRI (*Wolburg H et al., 2012*). The impact of the BBB on the detection of circulating biomarkers in gliomas has been investigated evaluating the relationship between MRI metrics reflecting BBB disruption and plasma cfDNA concentration in GBM patients. These studies suggest that cfDNA concentration and tumour volume are associated only in patients with high degrees of BBB disruption, suggesting that the release of nucleic acids dependents on the level of BBB permeability (*Nabavizadeh SA et al., 2020).* Recent studies also suggest that miRNAs can across the BBB and pass to the cerebrospinal fluid (CSF)

and blood as the content of brain released extracellular vesicles (Figure 7, *Müller Bark J et al., 2020*).

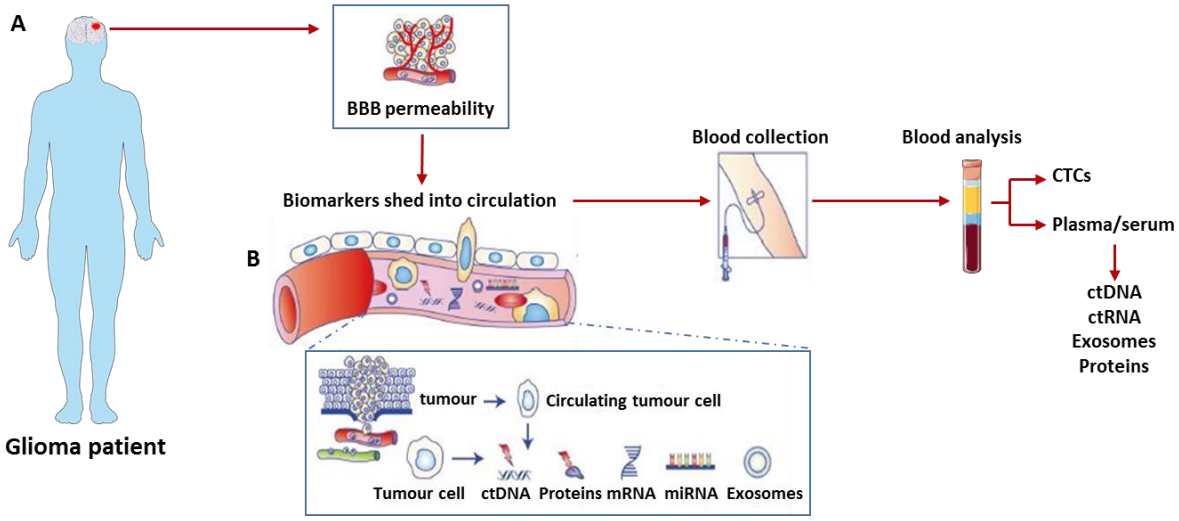

Figure 7: Representation of biomolecules release from the tumour mass via BBB into the bloodstream in glioma: (a) Glioma patients frequently have an altered BBB integrity (b) different type of biomolecules may enter the circulatory system from the breakdown of the tumour mass (Figure adapted from *Müller Bark J et al., 2020*).

- **Circulating microRNA**

MiRNAs are among the nucleic acid molecules that can be released from cells into biological fluids, in particular they can be secreted in association with protein complexes, which also include Argonaute proteins, or within extracellular vesicles (*Turchinovich A et al., 2011*) (Figure 8).

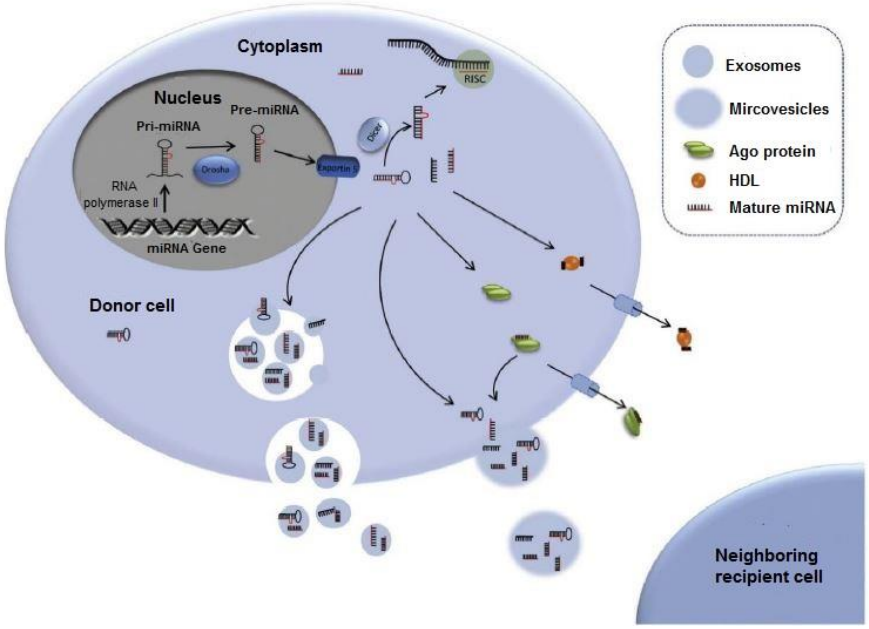

Figure 8: Mechanisms of miRNA secretion from the cell. MiRNA can be released from the cell in association with complex proteins, including Argonaut proteins or lipoproteins, or as the content of extracellular vesicles such as exosomes or microvesicles (Figure taken from *Sohel MH et al., 2016*).

Although the processes of microRNA secretion by cells are not yet elucidated in detail, there is evidence of the presence of regulatory mechanisms which determine the secretion of miRNAs based on specific characteristics. Villarroya-Beltri and colleagues described a mechanism of miRNA secretion within the exosomes regulated by the heterogeneous nuclear ribonucleoprotein A2/B1 (hnRNPA2B1) which would select the miRNAs based on specific motifs in their sequence (*Rooj AK et al., 2016; Sohel MH et al., 2016; Santangelo A et al., 2017*). The association of microRNAs with protein complexes or membrane-derived structures preserves their integrity within the biofluids. This feature, together with their small size, is at the basis of the greater stability of cell-free miRNAs compared to other types of circulating RNAs (*Mo MH et al., 2012*).

- **Circulating microRNA and Glioma**

The first evidence concerning the correlation between circulating miRNA levels and tumours dates back to the study carried out by Lawrie and colleagues, published in 2008, which allowed the identification of three microRNAs (miR-155, miR-210 and miR-21) whose expression was higher in the serum of patients with diffuse large B-cell lymphoma than in healthy individuals (*Lawrie CH et al., 2008*). These observations, combined with the particular stability of miRNAs in biofluids and their involvement in tumorigenesis, suggested the possibility of using these small RNAs as non-invasive biomarkers for tumours. In fact, in the last decade, there was a steady increase in the number of studies concerning circulating miRNAs in patients suffering from different types of cancer (*Larrea E et al., 2016).* MiR-21 is one of the most studied miRNAs in this research field, it is overexpressed in the plasma of glioblastoma patients compared to samples from healthy individuals. Its levels are also elevated in exosomes extracted from both serum and CSF of patients with grade IV glioma (*Santangelo A et al., 2017; Zhou Q et al., 2018; Wang Q et al., 2012*). These observations suggest the potential of this circulating miRNA as a diagnostic biomarker for glioblastomas. Through "genome-wide" techniques, that allow to analyse expression profiles of a large number of microRNAs (e.g., microarrays, NGS, etc), it is possible to identify specific groups of miRNAs, the so-called tumour signatures, whose expression is specifically altered in gliomas. The evaluation of a miRNA combination is often more specific and informative than the analysis of individual microRNAs, since it is widely recognized that single miRNA profiles may provide a low accuracy as cancer biomarkers, mostly due to the multifactorial nature of tumour but also to the large number of targets for a single miRNA (Yang *C et al., 2013*).

Experimental evidences suggest that the presence of extracellular microRNAs may have a functional role in tumour progression. The extracellular vesicles released by the tumour cells can indeed interact with the other non-tumoral cell types and free their load of macromolecules, including miRNAs, which in turn can influence and alter the characteristics and behaviour of these "recipient" cells (*Sohel MH et al., 2016*). The secretion of circulating miRNAs, as well as other types of macromolecules, could therefore represent a sort of paracrine signalling through which the tumour can influence the surrounding microenvironment, creating the conditions for the dissemination of cancer cells in the surrounding tissues (*Sohel MH et al., 2016*).

SCOPE OF THE RESEARCH PROJECT

Gliomas represent a medical challenge due to their anatomical location, diffuse, infiltrative growth, the resulting impact on brain functioning and their biological complexity. They encompass a range of different molecular subtypes, many of which have a well-defined profile of driver mutations. Among the key genetic events, the IDH mutation is noteworthy from both a diagnostic and a prognostic point of view. Tissue biopsies are essential to establish a diagnosis and a molecular profile. However, they are invasive procedures with a significant risk and they may only capture a static snapshot of the tumour, being useless for patient follow-up. A majority of gliomas inevitably recurs and monitoring the tumour burden of the recurrence is currently achieved by imaging, but it has limitations in assessing tumour burden, tumour infiltration into adjacent brain, and sometimes are unable to discriminate between tumour recurrence and pseudo-progression. Liquid biopsies, in contrast to tissues biopsies, have the advantage of being minimally invasive, allowing multiple sampling for disease monitoring, and potentially could provide, coupled with advanced molecular technologies, the possibility of assessing a wide landscape of molecular markers that the tumour sheds in body fluids. This allows a dynamic patient's management and a personalized medicine approach.

MiRNAs are deregulated not only in tumour tissues but also in biofluids, where they circulate in a very stable form, making them interesting candidate as biomarkers. Several circulating miRNAs have been evaluated in gliomas as single biomarkers but it is widely recognized that single miRNA profiles may provide a low accuracy as cancer biomarkers, mostly due to the multifactorial nature of tumour and to the large number of targets for a single miRNA. Thus, the evaluation of a multiple miRNA signature could be a more valuable and reliable approach for glioma patients' management.

The objective of this research was *a)* to identify a signature of serum miRNAs as a novel non-invasive tool for diagnosis and monitoring of glioma patients; *b)* to decipher their function in gliomas in terms of tumour behaviour.

MATERIALS AND METHODS

Patients and sample processing

This study was conducted using a training cohort that consisted of 37 glioma patients with tumours ranging from grade II to IV, recruited at the Regina Elena National Cancer Institute (IRE), which included, matched by gender and age, 27 patients with IDH wild-type and 10 patients with IDH mutated. The biological and clinical-pathological characteristics of the study participants are shown in Figure 1A of the Results section. An additional set of subjects was used to evaluate the miRNAs diagnostic accuracy. This second cohort consisted on 15 glioma patients and 15 healthy subjects matched by gender and age. For each patient, a blood sample was collected before surgery in BD Vacutainer serum tubes using a 21-gauge needle. Sampling method was consistent throughout the study to minimize any pre-analytical variables. The samples were kept at room temperature (RT) for 30 min to allow blood coating and then centrifuged at RT for 20 min at 1100×g, the supernatant was further centrifuged for 5 min at 1300×g. The serum was transferred into sterile cryovials and stored at −80 °C until further analysis.

In addition, samples of formalin-fixed, paraffin-embedded (FFPE) tumour tissue were analyzed for 28 patients.

Cells lines and culture conditions

SW1783 (astrocytoma grade III, IDH wild-type) and BT142 (oligoastrocytoma grade III, IDH mutant) human glioma cell lines were used for the experiments performed in this study. SW1783 was cultured in DMEM medium GlutaMAX™ Supplement (Gibco) supplemented with 10% heat-inactivated fetal bovine serum (FBS; Gibco), and 1% penicillin–streptomycin (P/S; Gibco). BT142 was grown in NeuroCult NS-A proliferation medium (Stem Cell Technologies) supplemented with 20ng/mL recombinant human Epidermal Growth Factor (EGF; PeproTech), 100 ng/mL recombinant human Platelet-Derived Growth Factor-AA (PDGF-AA; PeproTech), 20 ng/mL recombinant human Fibroblast Growth Factor (FGF; PeproTech) and 2 µg/mL heparan sulfate (Sigma). Both cell lines were cultured in a humidified atmosphere at 37 °C, 5% CO_2. For miRNA analysis in cells and related conditioned culture medium, cells were seeded and after 48 hours the medium was replaced with DMEM 2%FBS for SW1783 cell line, and NeuroCult Completed medium with 2% serum supplement for the BT142 cells. Culture medium was centrifuged at 1,000

x g for 10 minutes, the supernatant was further centrifuged at 2000 x g for 10 minutes, filtered using 0.22 μm polyether-sulfonate low-protein binding filters, aliquoted and stored at -80°C (*Bakr et al, 2018*).

RNA extraction from serum, tissue, cells and cell culture medium

Total RNA was extracted from 200 μl of serum or 400 μl of conditioned cell culture medium, and purified by a column-based method that includes small RNAs and minimize the carry-over of enzyme inhibitors typically contained in biofluids, using the miRNeasy Serum/Plasma Advanced Kit (Qiagen), in accordance with manufacturer's instructions. During the extraction process, a mixture of spike-in synthetic RNA was added inside the lysis buffer before adding it to the serum sample. RNA spike-in mix contains 52 synthetics 5'-phosphorylated miRNAs at different concentrations (QIAseq miRNA Library QC PCR Panel Kit, Qiagen). Since spectrophotometric methods, commonly used to establish the concentration of nucleic acids in a solution, do not allow to accurately determine the yield of RNA extracted from serum samples and no endogenous small RNA is recognized as suitable normalizer for circulating miRNA evaluation (*Li Y et al; 2012*), the results of subsequent analyzes have been normalized according to the starting serum volume.

Total RNA was isolated from cells (intracellular fraction) lysed in TRIsure™ (Bioline, Meridian Bioscience), according to manufacturer's instruction and eluted in 30 μl of RNase-free water.

FFPE samples were deparaffinated using a Deparaffination solution (Qiagen). Total RNA was isolated from FFPE tissue samples by the AllPrep DNA/RNA FFPE Kit (Qiagen), according to manufacturer's instructions.

RNA quantification from cells and tissue was done by NanoDrop ND-1000 spectrophotometer (ThermoFisher Scientific), measuring the absorbance at 260 nm wavelength.

Serum samples quality assessment

Reproducible RNA isolation may be difficult from some types of samples. Some RNA samples may contain compounds that alter the sample quality (such as nucleases) or inhibit the downstream enzymatic reactions, even though RNA has been purified using the best standard procedures. This may result in different efficiencies of the library preparation for NGS experiments. For that reason, it is necessary to control each sample before proceeding with the library preparation.

One way to check for variability in isolation efficiencies is by adding known RNA templates (Spike-ins) at the beginning of the extraction procedures prior to further analysis. The quality

assessment has been done by Reverse Transcription quantitative Polimerase Chain Reaction (RT-qPCR). To this purpose, miRNA molecules were reverse-transcribed into complementary DNA (cDNA). The synthesis of cDNA was carried out starting from 2 µl of the RNA solution extracted from the serum. For the reverse transcription the QIAseq™ miRNA Library QC PCR kit II (Qiagen) was used. The reaction took place by incubating the reaction mixture at a temperature of 42°C for 60 minutes, followed by an enzyme inactivation step at 95°C for 5 minutes, the samples were then cooled to 4°C and stored at -20°C until the further use. The synthetic RNA spike-in UniSp6 was added to the Reverse Transcription mixture as a quality control of cDNA synthesis reaction. The cDNA samples were subsequently analysed by qPCR using the miRCURY LNA SYBR Green PCR Kit (Qiagen). The reaction was carried out in triplicate for each sample using an ABI 7900 Real Time PCR System (Applied Biosystem) thermal cycler following an amplification cycle that includes: a first phase of 2 minutes at 95°C, followed by a succession of 40 2-step cycles at 95°C for 10 seconds and 60°C for 1 minute each, and a final dissociation stage. SDS v2.2.2 software was used for data processing.

For the evaluation of miRNAs extracted from serum, two synthetic RNA spike-ins, UniSp100 and UniSp101, were evaluated to check the consistency of samples extraction.
The typical Cq value (quantification cycle represents the number of cycle needed to reach a set threshold fluorescence signal level) is in the range of 31-34 for UniSp100 and 25-28 for UniSp101. The ΔCq between these two Spike-ins should be around 5-7. Moreover, UniSp6 cDNA synthesis control should display Cq values below 20.

Since hemolysis can alter circulating miRNA levels, a hemolysis test was introduced in the samples quality control procedure. To this end, the levels of miR-451, a particularly abundant miRNA in erythrocytes, were evaluated in the samples and compared with the amount of miR-23a, a miRNA not altered by hemolysis, based on the indications provided by the Qiagen protocols: samples in which the Cq values of miR-23a are five times or more than five times higher than the Cq values of miR-451 were considered hemolyzed and therefore discarded from the analysis *(Blondal T et al, Methods, 2013*).

Small RNA Next-Generation Sequencing and Library preparation

Next-Generation Sequencing technologies, also called massively parallel sequencing or just deep sequencing, are powerful platforms which have enabled the sequencing of thousands to millions of fragments of DNA or cDNA simultaneously. This powerful tool is revolutionizing fields such

as transcriptome profiling, personalized medicine and molecular diagnostics (*Wang Z et al., 2009; Ilyas M., 2017*). RNA-seq is essentially a massively parallel sequencing of RNA-derived cDNA which is able determine and record the sequence of coding RNA (mRNA) and also of different populations of ncRNA species, such as transfer RNA (tRNA), and small RNAs including Piwi-interacting RNAs (piRNAs), short interfering RNAs (siRNAs), microRNAs from different biological samples (*Costa-Silva J et al., 2017; Williams Z et al., 2013*).

For miRNA library preparation from serum samples, we used the recommended starting amount of 5 µL of total RNA isolated from 200 µl of serum. Then, we proceeded with library preparation using the QIAseq miRNA Library Kit (Qiagen) as indicated by the manufacturer's protocol. First, adaptors are ligated sequentially to the 3' and 5' ends of miRNAs. Adaptors include molecular bar codes called UMIs (Unique Molecular Indices), enabling unbiased and accurate miRNome-wide quantification of mature miRNAs by NGS. Subsequently, universal cDNA synthesis with UMI assignment, cDNA cleanup, library amplification and library cleanup are performed. Proprietary methodology using modified oligonucleotides virtually eliminates the presence of adapter dimers in the sequencing library, effectively removing a major contaminant often observed during sequencing. The kit is also designed to minimize the presence of hY4 Y RNA, which is often observed at high levels in serum and plasma samples. The following reactions are part of the workflow:

- 3' Ligation: A pre-adenylated DNA adapter is ligated to the 3' ends of all miRNAs.
- 5' Ligation: An RNA adapter is ligated to the 5' end of mature miRNAs.
- cDNA synthesis: The reverse transcription primer contains an integrated UMI. The RT primer binds to a region of the 3' adapter and facilitates conversion of the 3'/5' ligated miRNAs into cDNA while assigning a UMI to every miRNA molecule. During reverse transcription, a universal sequence is also added that is recognized by the sample indexing primers during library amplification.
- cDNA cleanup: After reverse transcription, a cleanup of the cDNA is performed using a streamlined magnetic bead-based method.
- Library amplification and cleanup

Yield and size distribution of resultant libraries were validated using Agilent 2100 Bioanalyzer on a High-sensitivity DNA Assay (Agilent Technologies). Libraries were then pooled with an equal proportion for multiplexed sequencing on the Illumina NextSeq550 (Illumina) platform.

Reverse transcription, RT-qPCR and droplet-digital PCR

Reverse transcription (RT) reaction was performed on 3 µl of total RNA extracted from serum and cell supernatant, or 50 ng extracted from cells and FFPE tissue, using the TaqMan MicroRNA Reverse Transcription Kit and a Custom TaqMan RT Primer Pool (ThermoFisher Scientific), according to the manufacturer's instruction. The Custom TaqMan RT Primer Pool was prepared by adding 25µL of each individual 5X RT primer into a 1.5 ml screw cap tube, drying down the tube in a speed vacuum at 50°C for ~1h, and resuspending in 100 µL nuclease free H_2O.

For miRNA detection through droplet-digital PCR (ddPCR) in serum, cell fraction and cell supernatant, the cDNA was diluted 1:6 and 8 µL were used to prepare a 22 µL reaction mix containing 1,1 µL of 2X ddPCR Supermix for Probes (Biorad) and 1,1 µL 20X TaqMan miRNA PCR primer probe set. The PCR mixes for each sample were loaded in a disposable cartridge (Biorad) together with 70 µL of droplet generation Oil (Biorad), and loaded in the QX200 droplet generator (Biorad). 40 µL of droplets were then transferred into a 96-well plate, the plate was heat-sealed with foil and then placed in a thermal cycler. An endpoint PCR was performed using the following conditions: 95°C for 10 minutes, then 40 cycles of 95°C for 15 seconds and 60°C for 1 minute, and a final step at 98°C for 10 minutes. After the PCR run, the 96-well plate was placed in the QX200 Droplet Reader for detection. The percentage of positive droplets was calculated by the software QuantaSoft (Biorad). MiRNA expression was analysed calculating copies of miRNA/µL.

For miRNA detection in tissue samples, TaqMan Universal Master Mix II, no UNG (ThermoFisher Scientific) was used for RT-qPCR. The reaction mix contained 1 µL of cDNA,

10 µL of TaqMan Universal Master Mix II no UNG, 1 µL 20X TaqMan miRNA PCR primer probe set and 8 µL H_2O nuclease-free. The reaction was carried out in triplicate for each sample using an ABI 7900 Real Time PCR System (Applied Biosystems) thermal cycler, following an amplification cycle which includes: a first phase of 2 minutes at 50°C, a second phase of 10 minutes at 95°C followed by a succession of 40 cycles at 95°C for 15 seconds and 60°C for 1 minute each. SDS v2.2.2 software was used for data processing. The obtained values were analyzed with the comparative ΔCt method normalizing according to the levels of snoRNA RNU44.

RNA quantification of SH3PXD2B (Forward 5'CCTTGACTTGGATGGTGATTC 3'; Reverse 5'TCTCTGCCTCATCTTTGGTG 3') was performed using SYBR Green-based qRT-PCR

(ThermoFisher Scientific). GAPDH (Forward 5' TCCCTGAGCTGAACGGGAAG 3'; Reverse 5'GGAGGAGTGGGTGTCGCTGT 3') gene expression was used as endogenous control. The reaction was carried out in triplicate for each sample using an ABI 7900 Real Time PCR System (Applied Biosystems) thermal cycler, as previously described.

Mimics transfection

Transfection is the introduction of nucleic acids into eukaryotic cells by nonviral delivery methods (Chahal et al., 2011). Various chemical or physical methods are used. SW1783 cell line was transfected with miR-1-3p, miR-26a-1-3p, miR-487b-3p mimics or negative control mimic, using the Lipofectamine RNAiMAX (Invitrogen). Invitrogen Lipofectamine RNAiMAX Transfection Reagent offers an advanced, efficient solution for siRNA or miRNA delivery. This technology is based on a cationic liposome formulation that functions by complexing with nucleic acid molecules, allowing them to overcome the electrostatic repulsion of the cell membrane and to be taken up by the cell (*Dalby MJ et al, 2004*).

Cells were transfected in suspension (150,000 cells/ml) according to manufacturer's instructions. In order to transfect cells with the three miRNA-mimics (hsa-miR-1-3p, hsa-miR-26a-1-3p, hsa-miR-487b-3p, Dharmacon) simultaneously, a final concentration of 0.5 nM was used for each one, reaching a total final concentration of mimic of 1.5 nM. Conversely, to assess the functional effects of the single miRNAs, 0.5 nM of the miRNA-mimic of interest was used, adding also 1 nM of negative control control (MirVana miRNA Negative control #1, Invitrogen), in order to respect the concentration ratio of mimics and ensure that observed results are not due to variations related to the different concentrations of oligonucleotides used in the transfections. For the same reasons, in the case of the negative control, the cells were directly transfected with a final concentration of 1.5 nM of MirVana miRNA Negative control #1 (Invitrogen). Cells were then plated at a density of 150,000 cells/ml in 6-well or 96-well plates and analysed 48h and 72h after transfection. Transfection efficacy was evaluated assessing the uptake of the fluorescent transfection indicator siGLO (Dharmacon) and by evaluatig miRNA expression through RT-qPCR.

Cell viability and proliferation

Cell viability was evaluated through standard cell counting using Trypan Blue (TermoFisher). Trypan Blue is recommended for use in dye exclusion procedures for viable cell counting. This method is based on the principle that live (viable) cells do not take up the blue dye, whereas dead

(non-viable) cells are permeable to it. Proliferation was assessed using the 3-(4,5-dimethylthiazol-2-yl)-2,5-diphenyltrazolium bromide (MTT) assay. The MTT assay is used to measure cellular metabolic activity as an indicator of cell viability, proliferation and cytotoxicity. This colorimetric assay is based on the reduction of a yellow tetrazolium salt (MTT) to purple formazan crystals by metabolically active cells. After solubilization, the absorbance of the formazan can be measured with a microplate absorbance reader. Cells were washed with PBS and then, DMEM with 10% MTT solution (Sigma-Aldrich) was added. After 3 hours (37°C) 100 µl of isopropanol solution was added. The absorbance was measured at 570 nm (microplate reader; Thermo Lab systems Multiskan EX).

Cell cycle and apoptosis analysis

Cell cycle was assessed by DNA content determination. Cells were permeabilized in a solution (0,1% Triton X-100, 0,1% sodium citrate) and stained with 50 µg/mL propidium iodide (PI), a fluorescent dye that binds stoichiometrically to the DNA. The stained material was then measured by flow cytometry using the BD LSR-Fortessa. Flow cytometry enables the identification of the cell distribution during the various phases of the cell cycle. Four distinct phases could be recognized in a proliferating cell population: the G0/G1-, S- (DNA synthesis phase), G2- and M-phase (mitosis, *Nunez et al., 2001*).

Apoptosis was evaluated by the Annexin V-FITC/PI Apoptosis Detection Kit (Invitrogen), according to the manufacturer's recommendations, using the flow cytometer BD LSR-Fortessa. Annexin V, conjugated to fluorescein isothiocyante (FITC), labels phosphatidylserine sites on the membrane surface of apoptotic cells, while PI labels cellular DNA in necrotic cells. This combination allows the differentiation among early apoptotic cells (annexin V positive, PI negative), necrotic cells (annexin V positive, PI positive), and viable cells (annexin V negative, PI negative).

Cell migration

Cell migration was determined through the Wound Healing assay. After 48h of transfection, cells were washed with PBS and DMEM supplemented with 2% FBS was added. Using a 10-µL sterile pipette tip, two scratches were created in each well. Next, the cells were placed into IncuCyte (Satorius) incubator during 48 hours. IncuCyte (Satorius) is an innovative platform which enable real-time live-cell imaging for visualization and quantification to better understand cells behaviour

and functions over time, by using continuous and automatically acquired images (*EssenBioscience, 2018*). In order to assess the cell migration, images of the wells were captured in five randomly selected microscopic fields in five different wells. The distance over which the cells had migrated into the denuded area was determined by measuring the wound width at 0 and 48 h using IncuCyte software to calculate the healing rate. Rate of cell migration was the result of dividing the distance of the width of the wound closure between the time considered (48h).

Luciferase assay

The target sites for miR-1-3p, miR-26a-1-3p or miR-487b-3p in human SH3PXD2B 3'UTR (NM_001017995.3) and its mutants were cloned into pGL3 Control vector (Promega) downstream of the luciferase gene. The mutant plasmids containing mutations of the miR-1-3p, miR-26a-1-3p and miR-487b-3p target sites were obtained by site specific mutagenesis. Human 293T cells were transiently co-transfected by Lipofectamine 2000 (Invitrogen), with 800 ng of firefly luciferase reporter plasmid containing wild-type or mutant SH3PXD2B 3'UTRs and of either the miRNA mimics hsa-miR-1, has-miR-26a-1 and has-miR-487b (20 pmol, Dharmacon) or control (Ctr)-mimics RNA oligonucleotides (20 pmol, ThermoScientificBio). Renilla luciferase vector (50 ng; pRL-TK vector) was co-transfected as an internal control to account for differences in transfection and harvest efficiencies. 48 h post-transfection cells were lysed and luciferase activity quantified using the Dual Luciferase Reporter kit (Promega Inc.), according to the manufacturer's instructions.

Bioinformatics and Statistics analysis

Data pre-processing were performed using QIAseq miRNA Primary Data Analysis pipeline, followed by sequences alignment to human genome using Bowtie 2 software. UMI counts were normalized by considering a size factor for each sample. To estimate the size factors, we considered the median of the ratios of observed counts to those of the spike-ins, whose counts can be obtained by considering the geometric mean of each gene across all samples (*Anders et al., 2010*). Then, to transform the observed counts to a common scale, the observed counts in each sample were divided by the corresponding size factor.

Differential expression analysis was performed using a Negative Bionomial Model. Linkage between the variance and the mean was established by a locally regressed non-parametric smooth

function of the mean. The Benjamini-Hochberg (BH) procedure for multiple testing was used to obtain adjusted P-values.

The Receiver Operative Characteristics (ROC) were used to determine the diagnostic accuracy of miRNAs in distinguishing glioma patients with IDH wild type from patients with IDH mutant (area under the ROC curve -AUROC - measures were selected to be ≥ 0.75). The diagram is a plot of the sensitivity (true-positive rate) vs specificity (false-positive rate) over all possible threshold values.

The Kaplan-Meier curves were used to estimate the overall survival (OS) and progression free survival (PFS) based on miRNA expression levels. Patients were stratified into high and low expression groups based on the miRNA expression z-score.

The miRWalk v3.0 database (http://mirwalk.umm.uni-heidelberg.de/) was used to identify the putative target transcripts of selected miRNAs as a comprehensive database that provides predicted as well as validated miRNA binding site information about the miRNAs of interest. A miRNA-mRNA inverse correlation analysis was then conducted for each transcript using the data available on the TCGA (https://cancergenome.nih.gov/) about a cohort of 448 patients with glioma with different IDH mutation status (IDH wild-type n=413, IDH mutant n=35). The list of putative targets was filtered considering transcripts with Spearman's rho correlation coefficient <-0.15 and p-value <0.05. A pathway analysis was then conducted using the KEGG, REACTOME and WikiPathways functional enrichment analysis.

RESULTS

Analysis of the global serum miRNA profiles in a cohort of glioma patients with different IDH status

To assess if circulating miRNAs could mirror the mutational status of IDH, the serum-miRNome of glioma patients was analyzed. Preoperative serum samples from a training cohort of 37 glioma patients with different IDH mutational status (n=27 IDH-wild type and n=10 IDH-mutant), matched by gender and age, were analyzed by small RNA-Sequencing (Figure 1 A, B). Based on the differential expression between IDH-wild type (IDH-wt) versus IDH mutant (IDH-mut) glioma patients, and the prognostic value, we selected a signature of 10 miRNAs deregulated between IDH-wt and IDH-mut patients. In particular, 8 miRNAs were downregulated (≥1.3 folds, adjusted p values ≤0.2) and 2 miRNAs were upregulated (≥1.4 folds; adjusted p values ≤0.2) in IDH-wt relative to IDH-mut samples (Figure 1C, D). The Kaplan-Meier curves of the entire 10 miRNA signature showed that the expression of these miRNAs is significantly and independently correlated with the PFS, both considering the miRNAs down-regulated in IDH-wt (hazard ratio: 0.24, 95% CI: 0.12-0.47 Figure 1E *left panel*) and those up-regulated (hazard ratio: 2.1, 95% CI: 1.16-3.83; Figure 1E *right panel*). For the prognostic evaluation we considered 34 out of 37 of the patients as the clinical information of three patients were not available.

A

Training cohort of 37 glioma patients used for small RNA-seq analysis		IDH-wt n=27	IDH-mut n=10
Age	mean	62	49
	range	24-77	29-77
Gender	males	17	7
	females	10	3
Grade	II/III	7	9
	IV	20	1

B

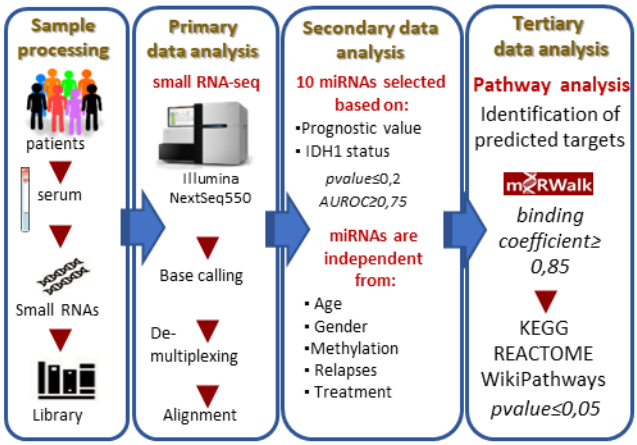

C

miRNA	IDH-wt vs IDH-mut	FC
miR-1-3p	↓	1,6
miR-26a-1-3p	↓	1,9
miR-127-3p	↓	1,7
miR-130b-5p	↓	1,3
miR-485-3p	↓	1,6
miR-487b-3p	↓	1,6
miR-493-5p	↓	1,7
miR-542-3p	↑	1,4
miR-589-5p	↓	1,3
miR-4778-5p	↑	1,7

D

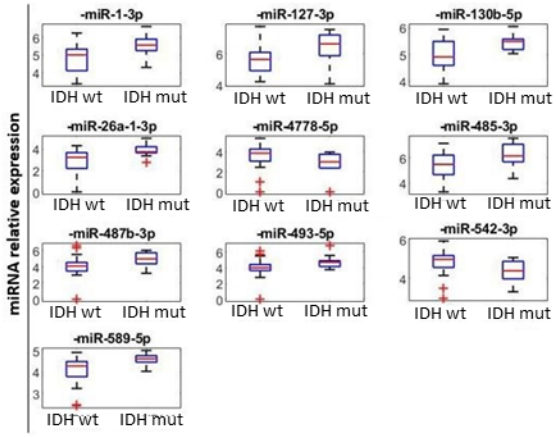

E

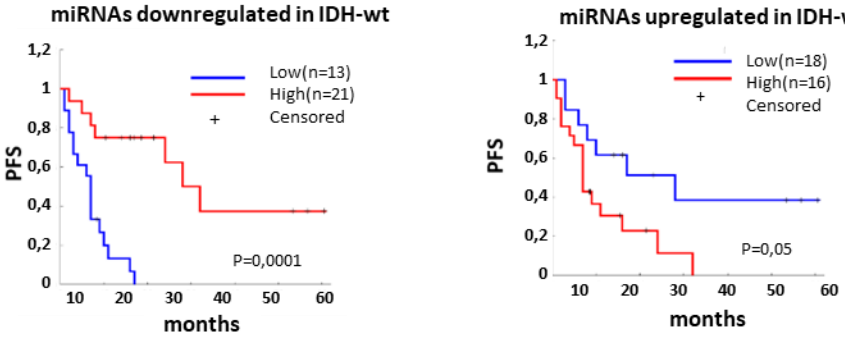

Figure 1. Identification by small RNA-seq of a circulating serum-miRNA signature as non-invasive biomarker. **A)** Clinic-pathological features of a training cohort of glioma patients with different IDH mutational status; **B)** Schematic representation of the experimental plan for the global miRNA profiling by small RNA-Seq; **C)** Selected serum miRNAs; **D)** Box-plots of miRNA expression levels. **E)** Kaplan-Meier curves for PFS based on miRNAs expression level (*right panel*: downregulated miRNAs in the IDH-wt group; *left panel*: upregulated miRNAs in the IDH-wt group). 3 patients dropped out. FC, Fold Change.

Evaluation of Diagnostic accuracy of the 10 serum-miRNAs signature

The ROC curves allow to obtain an estimation of the diagnostic accuracy, which is proportional to the area under the curve (AUC), and of the threshold value that maximizes the accuracy of the test (*Hajian-Tilaki K et al., 2013; Cerda J et al., 2012*; *Obuchowski N A et al., 2018*). Thus, to evaluate the diagnostic potential and discriminatory accuracy of the selected serum miRNAs in glioma patients, ROC curves were established. Our analysis revealed that the expression levels of each of the 10 selected serum miRNAs, showing an AUC value ranging from 0.75 to 0.86, were robust in discriminating patients with IDH-wt versus IDH-mut (Figure 2A). Different combinations of the selected miRNAs have been subsequently considered to evaluate if they could provide an improvement of the diagnostic accuracy. As shown in Figure 2B, the combination of miR-1-3p, miR-26a-1-3p and miR-487b-3p (patented: IT102021000005357), each one upregulated in IDH-mut subjects, led to a substantial improvement of the diagnostic performance (AUC 0.9), compared to each single miRNA of the signature, and is significantly correlated with both OS and PFS of glioma patients (Figure 2C).

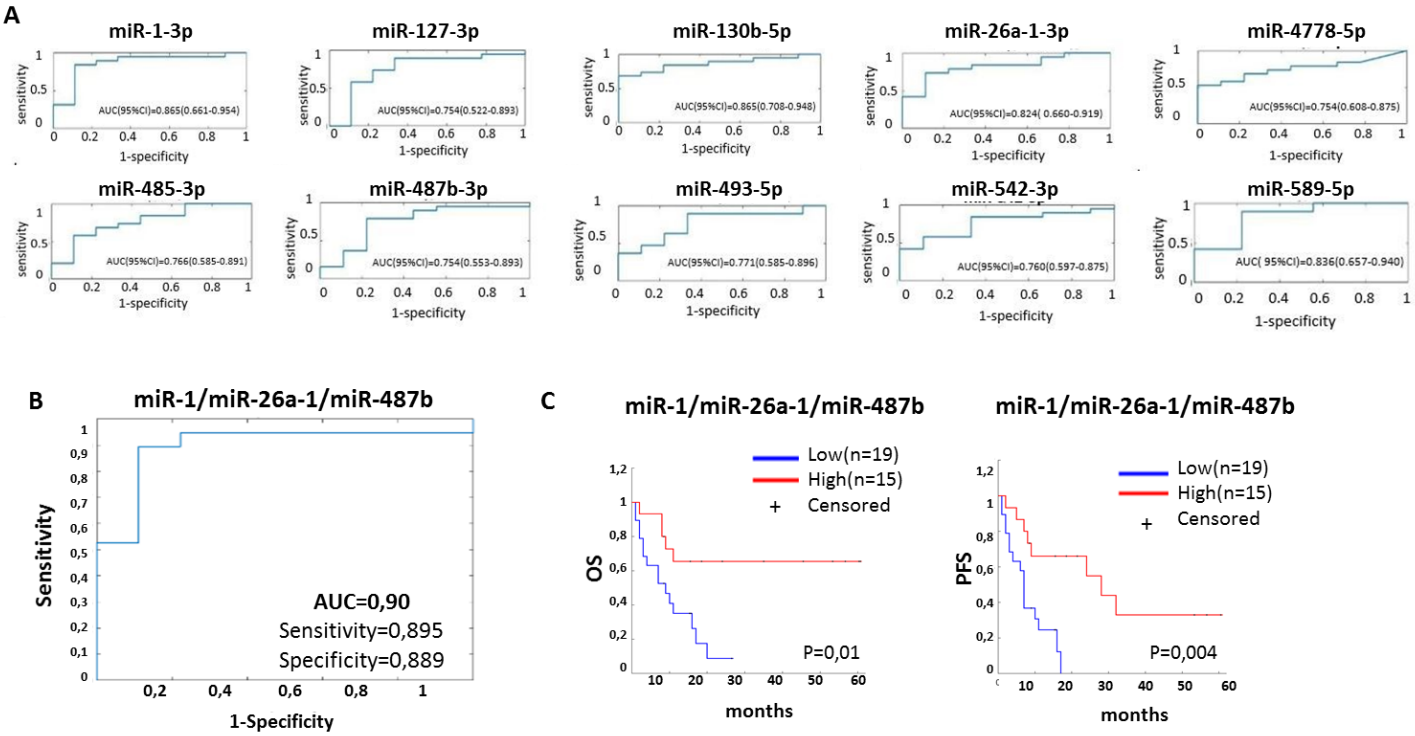

Figure 2. Roc curves to assess the diagnostic accuracy of the 10-miRNA signature.
A) ROC curves plotted for diagnostic potential and accuracy of the selected miRNAs in distinguishing IDH-wt from IDH-mut glioma patients. The corresponding AUC values are reported. AUC=Area Under the Curve, CI= Confidence Interval. **B)** ROC curve for miR-1/-26a-1/-487b combination improve AUC. **C)** Kaplan-Meier curves for OS and PFS based on miR-1/-26a-1/-487b expression levels.

To further confirm the diagnostic potential of our selected restricted signature (miR-1-3p, miR-26a-1-3p, miR-487b-3p), their expression was evaluated, by ddPCR, in serum samples of a new cohort of glioma patients and compared to, sex and age paired, healthy subjects. As indicated in Figure 3, the expression levels of miR-1-3p/ miR-26a-1-3p /miR-487b-3p are significantly downregulated in serum of glioma patients versus healthy controls.

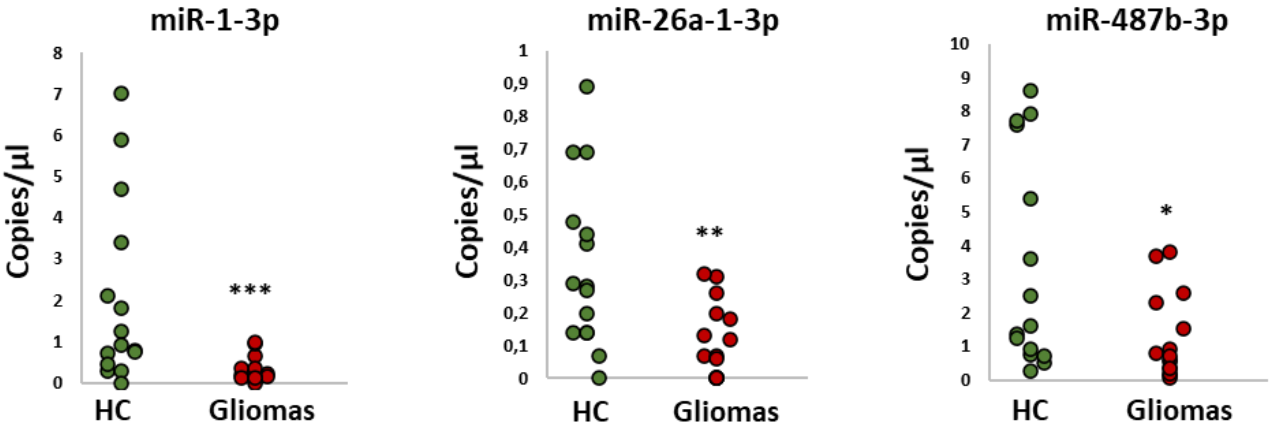

Figure 3. Expression levels of the three-serum miRNA signature in healthy controls and glioma patients. Scatter plots of the expression levels of the indicated miRNAs in serum samples of heathy subjects (controls; n=15) and glioma patients (gliomas; n=15) analysed by ddPCR. P-values (*** = P<0.001, ** =P<0.01, * =P<0.05) were calculated by Mann-Whitney test. HC, healthy controls.

Analysis of expression levels of miR-1, miR-26a-1 and miR-487b in tissue samples of glioma patients

As the comparison of the miRNA expression patterns between serum and tissues may provide additional evidence supporting the reliability of serum miRNAs as biomarkers, miRNA expression levels were further investigated in FFPE tissue biopsies of glioma patients. Our data, represented in Figure 4A, show a deregulation trend in the expression of the miR-1, miR-26a-1 and miR-487b signature in tissues of IDH-wt patients (n=16) compared to IDH-mut (n=12) samples. To support these data, we performed an *in silico* study based on RNA-seq data available on the TCGA dataportal on the three miRNAs expression levels in tumour tissue samples of glioma patients with different IDH mutation status (IDH-wt n=413, IDH-mut n=35) and in healthy controls (n=10). This analysis shows that miR-1 and miR-26a-1 are significantly down-regulated in IDH-wt versus IDH-mut (Figure 4B). On the other hand, expression levels of miR-1 and miR-487b are down-regulated in glioma versus healthy controls (Figure 4C). Altogether, our data suggest that the signature alteration in serum may reflect their changes in tumour.

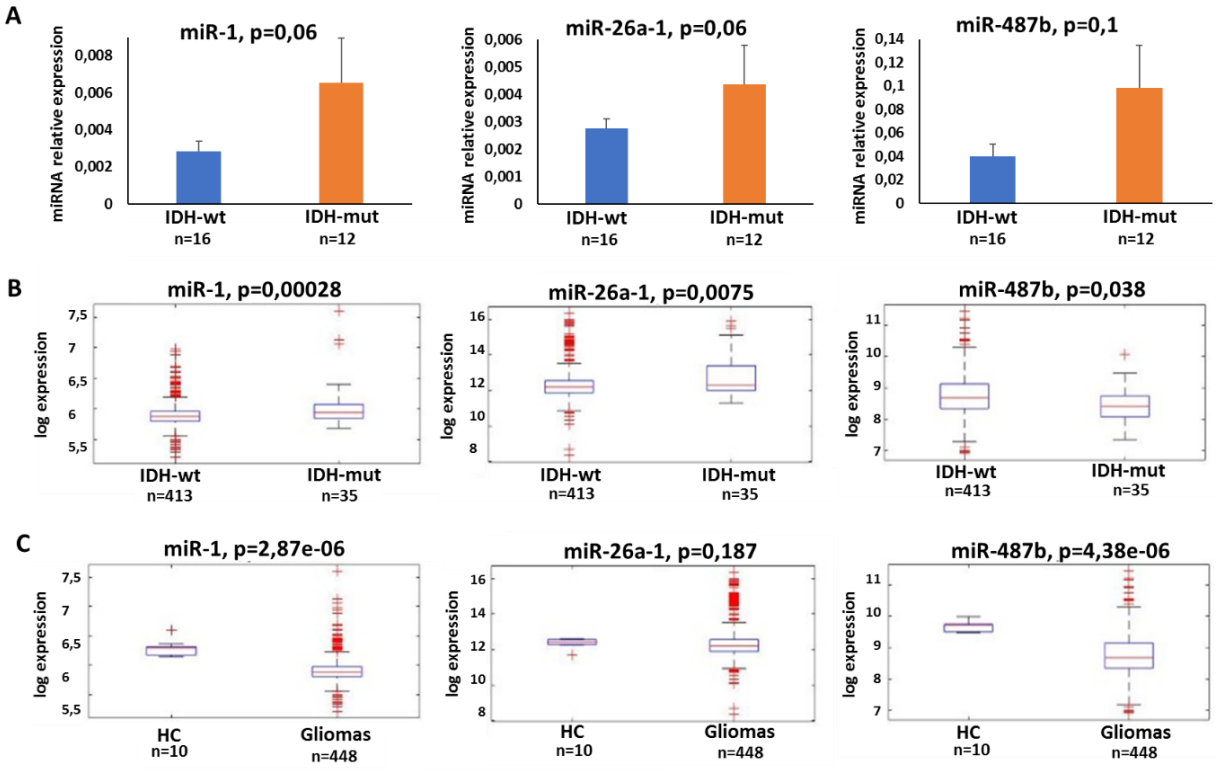

Figure 4. Expression levels of miR-1/-26a-1/487b in tissue samples of glioma patient.
A) Expression levels of the miRNA signature analysed by RT-qPCR in tissue of glioma patients with different IDH mutation status. Box plots based on TCGA datasets information of the indicated miRNAs in **B)** IDH-wt vs IDH-mut glioma patients and **C)** in Healthy Controls (HC) vs gliomas.

Analysis of the expression levels of miR-1/-26a-1/-487b in glioma cell lines with different IDH mutation status

To evaluate if glioma cell lines with different IDH mutation status can recapitulate what observed in glioma patients, the expression levels of miR-1/miR-26a-1/miR-487b were assessed in the cell fraction and in the paired extracellular conditioned medium of SW1783 (astrocytoma III, IDH-wt) and BT142 (oligoastrocytoma III, the only commercial IDH-mut glioma cell line available in the ATCC collection) glioma cell lines. The choice of these two cell lines (SW1783 and BT142 as counterpart) is due to the fact that although they have different IDH mutational status, both cell lines are grade III glioma. Figure 5 A, B show that the baseline expression level of the three-miRNA signature (miR-1/miR-26a-1/miR-487b) is up-regulated in the extracellular (supernatant) as well as in the intracellular (cells) fraction of IDH-mut cell lines. Moreover, it was also found that the value of extracellular to intracellular expression ratio for two out of three miRNAs is significantly higher in IDH-mut cells (Figure 5C). This means that IDH-mut cells present high

rates of miRNA release in the extracellular fraction. These data, in agreement with the results obtained in glioma patients, further confirm the *in-vivo* data

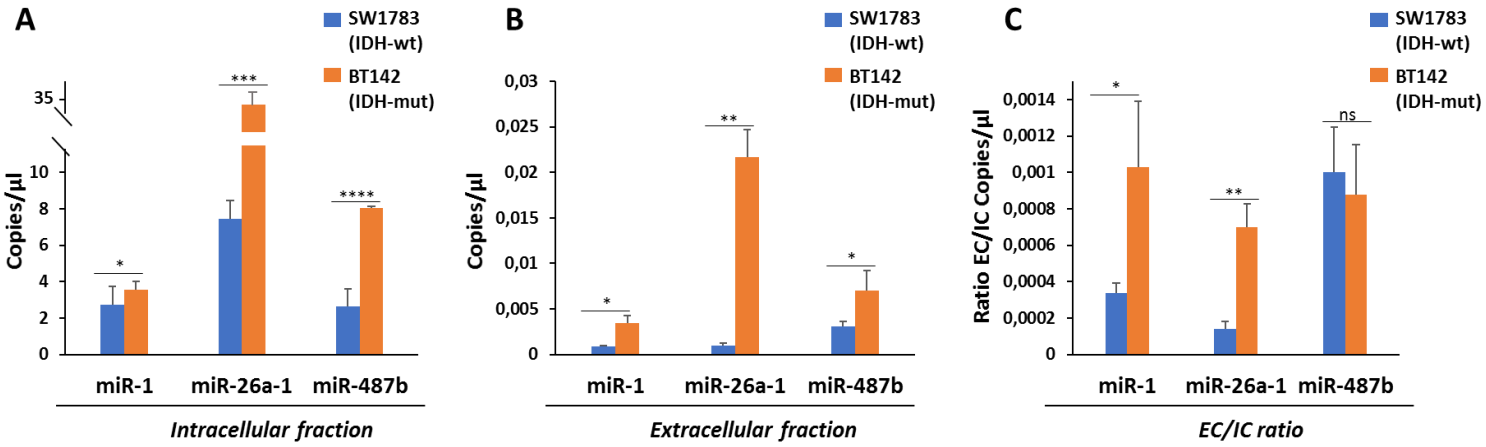

Figure 5. Expression levels of miR-1/-26a-1/-487b in glioma cell lines with different IDH mutation status. Evaluation by dPCR of the expression levels of the indicated miRNAs in the **A)** intracellular (cells) and **B)** extracellular (culture medium) fractions of IDH-wt and IDH-mut glioma cell lines. **C)** Ratio extracellular/intracellular (EC/IC) expression levels of miR-1/-26a-1/-487b (copies/ul) in IDH-wt (SW1783) and IDH-mut (BT142) glioma cells.

Study of the impact of combined expression of miR-1, miR-26a-1 and miR-487b on glioma behaviour

To get insights on the potential functional role of the selected miRNA-signature (miR-1, miR-26a-1, miR-487b) in the glioma behaviour, miRNA-gain-of-function strategies were performed. Since in our cohort miR-1/miR-26a-1/miR-487b are down-regulated in IDH-wt patients we overexpressed them, individually or in combination, in glioma IDH-wt cells using miRNA mimics and then we assessed their biological effects by cell viability (Trypan blue dye exclusion) and proliferation (MTT assay), apoptosis (flow cytometric determination of Annexin V), cell cycle profile (flow cytometric determination of cellular DNA content) and cell migration (wound healing assay performed using IncuCyte technology). As shown in figure 6A, the individual overexpression of the three miRNAs negatively affects the cell viability (*left panel*) and proliferation (*right panel*), but these effects are particularly pronounced with the combined overexpression of the three miRNAs. Next, cell apoptosis and cell cycle profiles were evaluated. We found that individual overexpression of miR-1, miR-26a-1 or miR-487b in IDH-wt glioma cells (SW1783) induced apoptosis, but the overexpression of the entire miRNA signature produced an increase of the apoptotic rate compared to each single miRNA (14,9 % miR-1, 14 % miR-26a-1, 14,6% miR-487b, 23% miRNA combination; Figure 6B). On the other hand, analysing the cell

cycle phases distribution, an increased number of events in G1/G0 phase was observed in cells overexpressing the three single miRNAs, suggesting an arrest of cell cycle elicited by each miRNA. Again, the effects on cell cycle arrest provoked by the combined overexpression of miR-1/miR-26a-1/miR-487b are noticeably increased respect to the single miRNA overexpression (Figure 6C). Finally, effects on cell migration were evaluated through the wound healing assay using the IncuCyte Technology. The results indicated that only the miR-1, but not the other two miRNAs of the signature (miR-26a-1 and miR-487b**),** is able to suppress the migration ability, leading to a 40% of reduction on the cell migration rate compared to the SW1783 cells transfected with the negative control (Figure 6D). These data reveal that the combined overexpression of miR-1/miR-26a-1/miR-487b, respect to the single miRNA, remarkably affects, even if not synergic, at a higher level several biological functions such as cell viability, proliferation, apoptosis and cell cycle arrest, suggesting that the use of this restricted miRNA signature reinforces, as a whole, the potential oncosuppressor role of its single members.

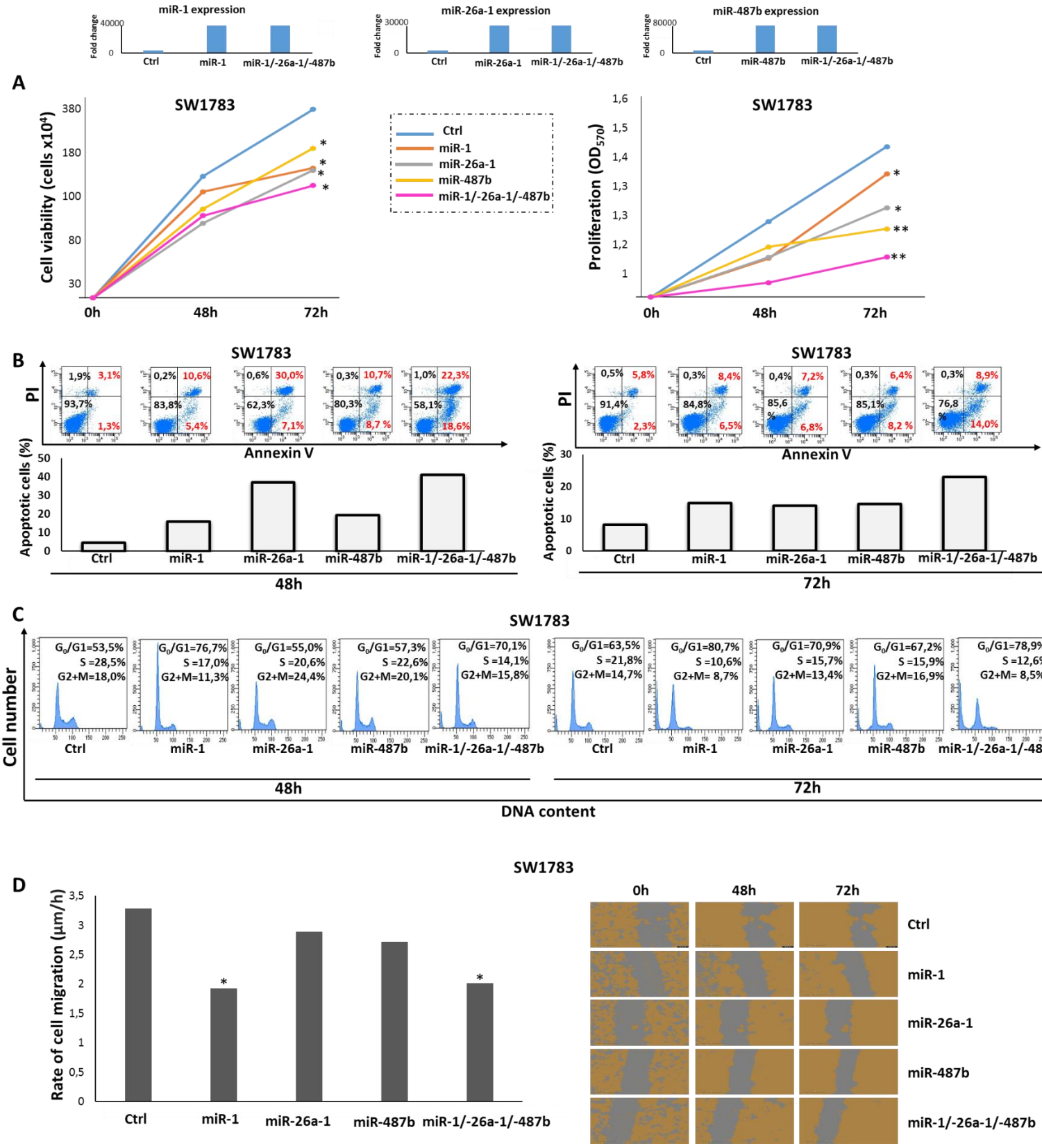

Figure 6. Biological effects of overexpression of miR-1/-26a-1/-487b in IDH-wt glioma cells.
Upper panel miRNA expression levels in SW1783, IDH-wt glioma cells, upon transfection in single or in combination of the indicated mimics. **A)** Cell viability (*right panel*), proliferation (*left panel*), assessed by Trypan Blue and MTT, respectively, after 48h and 72h of transfection with individually or combined indicated miRNA mimics. **B)** Apoptosis and **C)** cell cycle evaluated by FACS in SW1783 IDH-wt glioma cells after 48h and 72h of transfection with individual or combined indicated miRNA mimics. **D)** Cell migration evaluated by real-time live-cell imaging during 72 hours. *Right panel* shows the rate of cell migration and *left panel* shows representative images taken by the Incucyte.

Identification of miRNA targets and impacted signalling pathways

To gain more information on the miR-1, miR-26a-1 and miR-487b functional role we performed an in *silico analysis* of the miRNA signature putative target genes by the miRwalk database. From the resulting genes, we selected those which are targets of at least 2 out of the 3 miRNAs of the signature. Moreover, as the selected miRNAs depends on the presence of a IDH mutation, we performed an *in silico* analysis using a TCGA glioma cohort to identify predicted target genes differentially expressed between IDH-wt and IDH-mut patients (Fold change≥1.5). This combined analysis leads to the identification of 48 predicted targets down-regulated in IDH-mut vs IDH-wt patients that were used for functional annotation clustering by KEGG pathways, REACTOME and WikiPathways databases. We found that the miR-1/miR-26a-1/miR-487b signature targets are significantly enriched in several common pathways involved in biological processes altered in cancer, such as metabolism, cell proliferation, invasion, as well as in potentially targetable signaling pathways like the PI3K or the VEGF signalling pathways (Figure 7A; *Cancer Genome Atlas Research Network, 2008*). To narrow the analysis to a more manageable number of records, we further selected those targets which, in the TCGA glioma dataset, were inversely and significantly correlated with at least 2 out of 3 miRNAs of the signature. Finally, 15 predicted targets were selected (Figure 7B). Interestingly, for some of them a role in gliomas has been described such as *ANGPT2, EMP1, FAM46A, HOXB3, IKBIP, MCM10, RAP2B, RCC1, ZFP36L2* (*Zhang L et al., 2018; Wang J et al., 2019; Xu K et al., 2018; Yang Y et al., 2021; Miao F et al., 2019; Che Mat MF et al., 2021*).

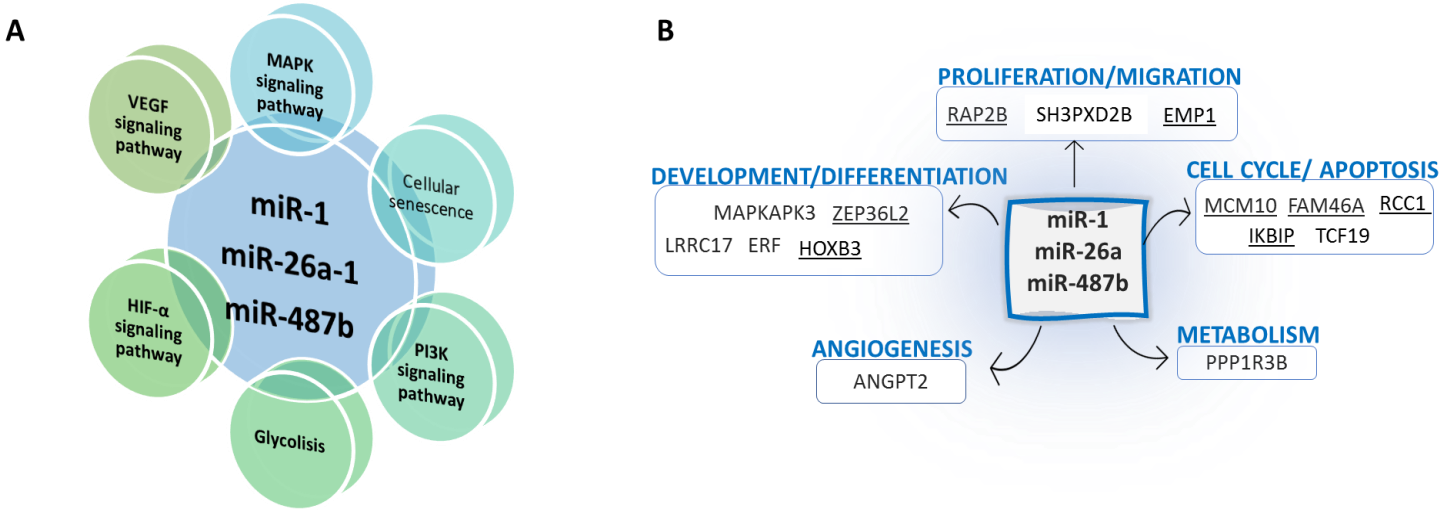

Figure 7. Schematic representation of the pathways and target analyses of the restricted miRNA signature.
A) Enriched pathways impacted by the predicted targets. **B**) Predicted targets selected from the *in silico* analyses. Underlined genes already described in glioma.

To validate these putative miRNA targets, first we evaluated the binding score between the 3'UTR of the selected 15 genes and the seed sequence of the miRNA signature members. The best matches 3'UTR-miRNA seed of all the three miRNAs was found for *SH3PXD2B* gene, a tyrosine kinase which encode for a TSK4 protein, involved in cell adhesion and migration (Figure 8A, *Kui et al., 2021*). For this reason, we initially focused on this predicted target gene by evaluating the *in vivo* consequences of miR-1, miR-26a-1 or miR-487b overexpression on SH3PXD2B mRNA levels. To this purpose we ectopically expressed the miR-1, miR-26a-1 and miR-487b, individually, into IDH-wt glioma cells constitutively expressing the target gene, then changes in the SH3PXD2B mRNA expression levels were evaluated by real-time PCR. We found that ectopic expression of miR-1 and miR-487b, but not miR-26a-1, caused a decrease in SH3PXD2B mRNA expression levels, (Figure 8B). Thus, to experimentally assess the direct interactions between the miR-1, miR-26a-1 or miR-487b and SH3PXD2B target gene, its human 3'UTR fragments with or without miR-1, miR-26a-1 or miR-487b binding site sequences (one putative binding site for each member of the miRNA signature; Figure 8A) were cloned downstream of the firefly luciferase reporter gene. As shown in Figure 8C, the relative luciferase activity of the reporter with wild-type 3'UTR was suppressed upon co-transfection with mimics miR-1 or miR-487b, whereas the respective deletion mutant reporters were not. No suppression of the luciferase activity was reported after co-transfection with mimic miR-26a-1. These data confirm that miR-1 and miR-487b, but not miR-26a-1 (Figure 8B, C) have a direct interaction with their respective binding sequences in the 3'UTR of the target gene. On-going experiments are now performed to evaluate the combined effect of the three miRNAs on mRNA levels, as well as individually or combined effects of the miRNA signature on SH3PXD2B protein levels.

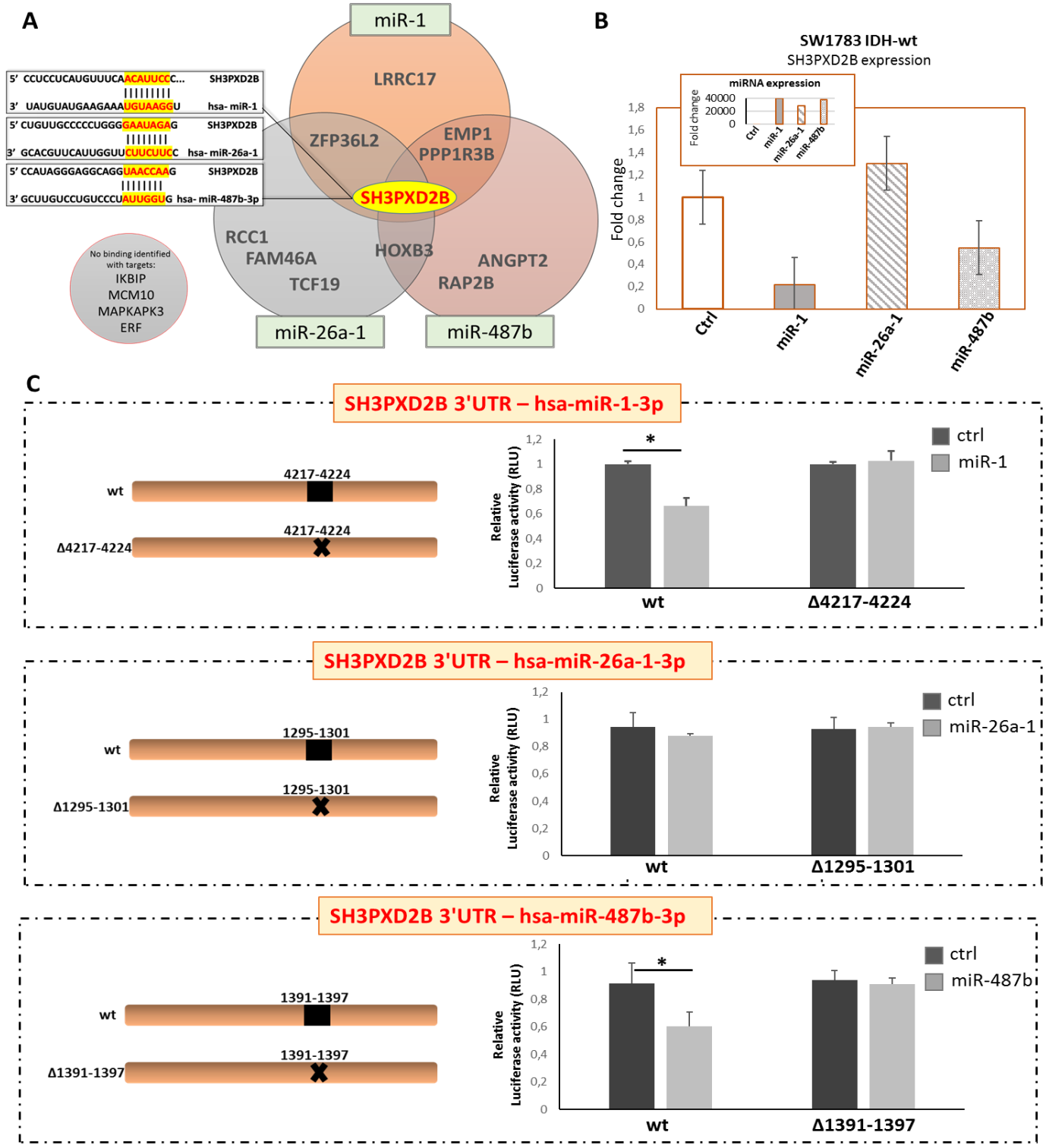

Figure 8. Identification of SH3PXD2B as direct target of miR-1 and miR-487b.
A) Venn diagram represents targets with a perfect binding site (at least 5 bases) between 3'UTR of indicated gene and the seed of the indicated miRNAs. **B)** (*upper panel*) expression levels of the miRNA signature after transfection with mimics. (*Lower panel*) SH3PXD2B mRNA expression levels in SW1783 IDH-wt glioma cells after miRNAs overexpression. **C)** *left panel:* schematic representation of reporter constructs containing the complete (3'UTR wt) or deletion mutants (Δ4217-4224, Δ1295-1301, Δ1391-1397) of miR-1, miR-26a-1 or miR-487b binding sequences in SH3PXD2B constructs used to measure luciferase activity. *Right panel*: Firefly luciferase activity in Human 293T recipient cells after transient co-transfection with *Renilla* luciferase *pRL-TK* of firefly luciferase reporter plasmid containing wild-type or the indicated deleted SH3PXD2B 3'UTRs and the mimic or ctrl-mimic miRNA. Firefly luciferase activity of each sample was normalized by Renilla luciferase activity. Results are expressed as fold activation relative to the basal activity of pGL3 empty Control vector (control). The normalized luciferase activity, set as mean of at least three independent experiments done in duplicate, is shown. Error bars represent the mean±s.e.m(n=3). *P value ≤0.05 (Student's t-test).

DISCUSSION

Gliomas represent a medical challenge due to their anatomical location, diffuse, infiltrative growth, the resulting impact on brain functioning and their biological complexity (*McFaline-Figueroa JR et al., 2018*; *Molinari E et al., 2019*). Nowadays stratification of tumour types is based on several genetic and epigenetic characteristics of the tumour with both diagnostic and prognostic value. In all mainstream settings, molecular markers are tested on neuropathologically assessed, and thus validated, starting material. This approach is of course limited in those patients with increased risk from a biopsy, due to the tumour location, the clinical performance status, or comorbidities (*Molinari E et al., 2019*). To overcome these barriers, liquid biopsies, in contrast to tissues biopsies, have the advantage of being minimally invasive, allowing multiple sampling for disease monitoring, and potentially provide, coupled with advanced molecular technologies, the possibility of assessing a wide landscape of molecular markers that the tumour sheds in body fluids. This allows a dynamic patient's management and a personalized medicine approach (*Larrea E et al., 2016; Siravegna G et al., 2019*). The identification of non-invasive markers, therefore, represents an important goal for improving the diagnosis and treatment of this type of cancer. Thus, the search for circulating biomarkers in the blood has become a field of study on which the interest of the scientific community has been directed. However, the presence of BBB must be considered when dealing with circulating molecules as brain tumour markers. The BBB integrity is often compromised in gliomas with different degrees of disruption in different stages and grades. In fact, several data suggest that the reliability of circulating molecules as biomarkers are dependent on the level of BBB permeability (*Nabavizadeh SA et al., 2020*; *Bruno DCF et al., 2020; Wolburg H et al., 2012*). However, even if a majority of diffuse gliomas, in particular GBM, almost invariably have a disrupted BBB, and a more generous release of circulating biomarkers would be expected (*Müller Bark J et al., 2020*) many aspects of the BBB impact on liquid biopsy are still unknown, thus more studies are required about this issue. Among the circulating molecules, the miRNAs are the most investigated as biomarkers mainly due to their frequent alteration in cancer and their high stability in biofluids (*Lawrie CH et al., 2013, Mitchell PS et al., 2008; Valihrach L et al., 2020*). This category of transcripts is frequently deregulated in biofluids of glioma patients and, with a range of ~30-99 % sensitivity and ~70-100 % specificity, holds promise for a potential disease detection (*Diaz Mendez AB et al., 2021*). Despite the large number of miRNAs examined as biomarkers, only few of them have yielded consistent results across different studies. This high

variability limits their usefulness as non-invasive biomarkers and could be explained by differences in study design, sample size, ethnicity, and methodology used (*Zhi F et al., 2015*). Another limitation is the lack of miRNA association to molecular features since, despite the 2016 update of the WHO classification, up today few articles evaluate correlation of miRNA profiles with relevant molecular markers (*Ebrahimkhani S et al., 2018; Zhong F et al., 2019; Zhang H et al., 2019; Zhang Y et al., 2019*). Moreover, it is widely recognized that single miRNA profiles may provide a low accuracy as cancer biomarkers, mostly due to the multifactorial nature of tumour and to the large number of targets for a single miRNA. However, to date only few comprehensive analyses of the entire serum miRNA repertoire in glioma patients has been performed (*Ebrahimkhani et al., 2018*).

In this doctoral thesis, using unbiased high-throughput next-generation sequencing and an integrative bioinformatics pipeline, we have identified a 10-serum miRNA signature with a prognostic value that discriminates IDH-wt from IDH-mut glioma patients with high specificity and sensitivity. We also found that, among the 10 identified miRNAs, the combination of miR-1-3p, miR-26a-1-3p and miR-487b-3p led to an improvement of the diagnostic performance, compared to each single miRNA. This restricted three-miRNA signature is significantly correlated with both OS and PFS and allows to discriminate glioma patients from healthy subjects. Moreover, we have also demonstrated that the combination of all these three miRNAs acts as tumour suppressor in IDH-wt glioma cells by exerting an increased adverse effect on cell viability, proliferation and migration, and by inducing apoptosis and cell cycle arrest. Previous studies have shown that these three miRNAs (miR-1-3p, miR-26a-1-3p and miR-487b-3p) have an impact on various aspects of glioma biology. MiR-1-3p has been described as tumour suppressor in many types of cancer, including glioma, as it inhibits the epithelial mesenchymal transition by directly targeting fibronectin (*Bronisz A et al., 2014; Liu J et al.,2019*), miR-26a-1-3p has been demonstrated to be involved in response to treatment in glioma cells (*Ge et al*, 2018) and miR-487b-3p has been found downregulated in GBM compared to non-neoplastic tissue (*Benetatos et al., 2013*). Furthermore, through *in silico* analyses we have identified a series of genes that are potential targets of two out of the three miRNA signature members and that, in addition, are differentially expressed in glioma patients with different IDH mutational status. Functional pathways analyses show that the identified targets are highly associated with important common signalling pathways related to brain cancer such as, PI3K-AKT, VEGF and MAPK signalling

pathways (*Cancer Genome Atlas Research Network, 2008*). PI3K-AKT is one of the core pathways in glioma tumorigenesis, showing alterations in the 88% of gliomas. PI3Ks-AKT signalling pathway is central to cell survival, growth, and proliferation (*Cheng KC et al., 2009*). In addition, hyperactivation of MAPK signalling pathway has been observed in glioma, impacting multiple tumorigenic processes such as proliferation, survival and migration. Moreover, mutations in at least one member of the pathway are found in the 83% of all glioma cases (*Daniel PM et al., 2018*). Among the predicted miR-1/miR-26 and miR-487 targets, we found that *SH3PXD2B*, showing the best 3'UTR-seed sequence pairing, is a direct novel target of the two members of our signature (miR-1 and miR-487b). This gene is a tyrosine kinase which has been demonstrated to promote intravascular and extravascular invasion and metastasis of hepatocellular carcinoma, human colon cancer, breast cancer, and melanoma cells (*Kui et al., 2021*). The protein product of the *SH3PXD2B* gene is known as TSK4, which plays an important role in the formation of functional podosomes and invadopodia of cells, and is required for the production of reactive oxygen species (ROS) by tumor cells. TSK4 is also involved in EGF signalling by regulating the actin cytoskeleton via Src and EGFR (*Dülk M et al, 2018*). Although there is no information on whether *SH3PXD2B* has an impact on glioma behaviour, it is known that this kinase forms a complex with the well-known Src kinase (*Dülk M et al*, 2018) whose activity is often aberrantly upregulated in glioma, promoting cell proliferation and migration and being connected to tumour progression, neoangiogenesis, and metastatization. Indeed, many clinical trials are focused the use of Src inhibitors for glioma treatment (*Cirotti C et al., 2020*). This suggests that SH3PXD2B could be considered as a potential 'druggable' target in glioma.

Conclusions

This thesis study highlights the potential for miRNA profiles to be used for glioma subtyping and grading on the basis of clinically relevant molecular markers (IDH). In particular, it suggests that the detection of a restricted serum miRNA signature, obtainable with minimal invasiveness via a simple blood withdrawal, holds great promises as biomarker to aid diagnosis and prognosis and may be used for the early identification and monitoring of relapses, for assessing therapy response of gliomas and discriminating progression from pseudo-progression, with the possibility of identifying subgroups of patients responsive to alternative therapeutic approaches. However, the assessment of the identified serum miRNAs in larger longitudinal cohorts of glioma patients are required to definitely determine their utility in clinical practice, and these studies are currently

underway. These findings have significant potential to transform the current diagnostic paradigms, as well as to provide distinct surrogate endpoints for clinical trials and thus can be considered a pathway towards personalized medicine.

BIBLIOGRAPHY

1. Acunzo M, Romano G, Wernicke D, Croce CM. MicroRNA and cancer--a brief overview. *Adv Biol Regul. 2015*; 57: 1-9.
2. Ahir BK, Ozer H, Engelhard HH, Lakka SS. MicroRNAs in glioblastoma pathogenesis and therapy: A comprehensive review. *Crit Rev Oncol Hematol. 2017*; 120:22-33.
3. Altwairgi AK, Raja S, Manzoor M, Aldandan S, Alsaeed E, Balbaid A, *et al*. Management and treatment recommendations for World Health Organization Grade III and IV gliomas. *Int J Health Sci (Qassim).* 2017; 11(3):54-62.
4. Anders S, Huber W. Differential expression analysis for sequence count data. *Genome Biol. 2010*; 11(10):R106.
5. Arvold ND, Lee EQ, Mehta MP, *et al.* Updates in the management of brain metastases. *Neuro Oncol. 2016*; 18(8):1043-1065.
6. Bakr S, Simonson B, Danielson KM, Das S. Extracellular RNA Isolation from Cell Culture Supernatant. *Methods Mol Biol. 2018*;1740:23-34.
7. Ballabh P, Braun A, Nedergaard M. The blood-brain barrier: an overview: structure, regulation, and clinical implications. *Neurobiol Dis. 2004*;16(1):1-13.
8. Barnholtz-Sloan JS, Ostrom QT, Cote D. Epidemiology of Brain Tumors. *Neurol Clin. 2018*; 36(3):395-419.
9. Bady P, Sciuscio D, Diserens AC, Bloch J, van den Bent MJ, Marosi C, *et al*. MGMT methylation analysis of glioblastoma on the Infinium methylation BeadChip identifies two distinct CpG regions associated with gene silencing and outcome, yielding a prediction model for comparisons across datasets, tumor grades, and CIMP-status. *Acta Neuropathol. 2012*; 124(4):547-60.
10. Bagley SJ, Nabavizadeh SA, Mays JJ, Till JE, Ware JB, Levy S *et al.* Clinical Utility of Plasma Cell-Free DNA in Adult Patients with Newly Diagnosed Glioblastoma: A Pilot Prospective Study. *Clin Cancer Res. 2020*; 26:397-407.
11. Belter A, Rolle K, Piwecka,M. Fedoruk-Wyszomirska A, Naskręt-Barciszewska MZ, Barciszewski J. Inhibition of miR-21 in glioma cells using catalytic nucleic acids. *Sci Rep.2016*; 6, 24516.

12. Banelli B, Forlani A, Allemanni G, Morabito A, Pistillo MP, Romani M. MicroRNA in Glioblastoma: An Overview. *Int J Genomics. 2017*; 2017:7639084.
13. Benetatos L, Hatzimichael E, Londin E, Vartholomatos G, Loher P, Rigoutsos I, *et al.* The microRNAs within the DLK1-DIO3 genomic region: involvement in disease pathogenesis. *Cell Mol Life Sci. 2013*; 70(5):795-814.
14. Bhaskaran M, Mohan M. MicroRNAs: history, biogenesis, and their evolving role in animal development and disease. *Vet Pathol. 2014*; 51(4):759-74.
15. Beyer S, Fleming J, Meng W, Singh R, Haque SJ, Chakravarti A, *et al*. The Role of miRNAs in Angiogenesis, Invasion and Metabolism and Their Therapeutic Implications in Gliomas. *Cancers (Basel). 2017*; 9(7). pii: E85.
16. Blondal T, Jensby Nielsen S, Baker A, Andreasen D, Mouritzen P, WrangTeilum M, *et al.* Assessing sample and miRNA profile quality in serum and plasma or other biofluids. *Methods. 2013*; 59:S1–6.
17. Boisselier B, Gállego Pérez-Larraya J, Rossetto M, Labussière M, Ciccarino P, Marie Y, *et al.* Detection of IDH1 mutation in the plasma of patients with glioma. *Neurology. 2012*; 79(16):1693-8.
18. Bronisz A, Wang Y, Nowicki MO, Peruzzi P, Ansari K, Ogawa D, *et al*. Extracellular vesicles modulate the glioblastoma microenvironment via a tumor suppression signaling network directed by miR-1. *Cancer Res. 2014*;74(3):738-750.
19. Bruno DCF, Donatti A, Martin M, Almeida VS, Geraldis JC, Oliveira FS, *et al*. Circulating nucleic acids in the plasma and serum as potential biomarkers in neurological disorders. Braz J *Med Biol Res. 2020*; 53(10):e9881.
20. Calin GA, Dumitru CD, Shimizu M, Bichi R, Zupo S, Noch E, *et al*. Frequent deletions and downregulation of micro-RNA genes miR15 and miR16 at 13q14 in chronic lymphocytic leukemia. *Proc Natl Acad Sci USA. 2002*; 99:15524–29.
21. *Cancer Genome Atlas Research Network*. Comprehensive genomic characterization defines human glioblastoma genes and core pathways. *Nature. 2008*;455:1061-8.
22. Capper D, Weissert S, Balss J, Habel A, Meyer J, Jäger D *et al.* Characterization of R132H mutation-specific IDH1 antibody binding in brain tumors. *Brain Pathol. 2010*; 20: 245-254.
23. Capper D, Jones D, Sill M Hovestadt V, Schrimpf D, Sturm D *et al*. DNA methylation-based classification of central nervous system tumours. *Nature .2018*; 555, 469–474.

24. Cerda J, Cifuentes L. Uso de curvas ROC en investigación clínica: Aspectos teórico-prácticos [Using ROC curves in clinical investigation: theoretical and practical issues]. *Rev Chilena Infectol. 2012*; 29(2):138-41.
25. Che Mat MF, Mohamad Hanif EA, Abdul Murad NA, Ibrahim K, Harun R, Jamal R. Silencing of ZFP36L2 increases sensitivity to temozolomide through G2/M cell cycle arrest and BAX mediated apoptosis in GBM cells. *Mol Biol Rep. 2021*.
26. Chen R, Smith-Cohn M, Cohen AL, Colman H. Glioma Subclassifications and Their Clinical Significance. *Neurotherapeutics. 2017*; 14(2):284-297.
27. Chen X, Zhang M, Gan H Wang H, Lee JH, Fang D *et al*. A novel enhancer regulates MGMT expression and promotes temozolomide resistance in glioblastoma. *Nat Commun. 2018*; 9, 2949.
28. Cheng CK, Fan QW, Weiss WA. PI3K signaling in glioma--animal models and therapeutic challenges. *Brain Pathol. 2009*; 19(1):112-20.
29. Cirotti C, Contadini C, Barilà D. SRC Kinase in Glioblastoma News from an Old Acquaintance. *Cancers (Basel*). 2020;12(6):1558.
30. Coolen M, Bally-Cuif L. MicroRNAs in brain development and physiology. *Curr Opin Neurobiol. 2009*; 19(5):461-70.
31. Costa-Silva J, Domingues D, Lopes FM. RNA-Seq differential expression analysis: An extended review and a software tool. *PLoS One. 2017*; 12(12):e0190152.
32. Dalby MJ, Riehle MO, Sutherland DS, Agheli H, Curtis AS. Use of nanotopography to study mechanotransduction in fibroblasts--methods and perspectives. *Eur J Cell Biol. 2004*;83(4):159-69.
33. Da Sacco L, Baldassarre A, Masotti A. Bioinformatics tools and novel challenges in long non-coding RNAs (lncRNAs) functional analysis. *Int J Mol Sci. 2012*; 13(1):97-114.
34. Daniel PM, Filiz G, Tymms MJ, Ramsay RG, Kaye AH, Stylli SS, *et al.* Intratumor MAPK and PI3K signaling pathway heterogeneity in glioblastoma tissue correlates with CREB signaling and distinct target gene signatures. *Exp Mol Pathol. 2018*;105(1):23-31.
35. Deng L, Xiong P, Luo Y, Bu X, Qian S, Zhong W, *et al*. Association between IDH1/2 mutations and brain glioma grade. *Oncol Lett. 2018*; 16(4):5405-5409.
36. Di Leva G, Garofalo M, Croce CM. MicroRNAs in cancer. *Annu Rev Pathol. 2014*; 9: 287-314.

37. Diaz Mendez AB, Tremante E, Regazzo G, Brandner S, Rizzo MG, Time to focus on circulating nucleic acids for diagnosis and monitoring of gliomas: a systematic review of their role as biomarkers, *Neuropathology and Applied Neurobiology, 2021*;47(4):471-487.
38. Dülk M, Szeder B, Glatz G, Merő BL, Koprivanacz K, Kudlik G, *et al.* EGF Regulates the Interaction of Tks4 with Src through Its SH2 and SH3 Domains. *Biochemistry. 2018*;57(28):4186-4196.
39. Ebrahimkhani S, Vafaee F, Hallal S, Wei H, Lee MYT, Young PE *et al*. Deep sequencing of circulating exosomal microRNA allows non-invasive glioblastoma diagnosis. *NPJ Precis Oncol. 2018*; 2: 28-018-0071-0.
40. Essen BioScience. Live-cell analysis inside your incubator. IncuCyteS3 live-cell analysis system.Manufacturer's brochure. *Essen BioScience, Ann Arbor, MI. 2018.*
41. Eulalio A, Behm-Ansmant I, Schweizer D, Izaurralde E. P-body formation is a consequence, not the cause, of RNA-mediated gene silencing. *Mol Cell Biol. 2007*; 27(11):3970-81.
42. Eulalio A, Huntzinger E, Izaurralde E. Getting to the root of miRNA-mediated gene silencing. *Cell. 2008*; 11, 132(1):9-14.
43. Figueroa JM, Skog J, Akers J, Li H, Komotar R, Jensen R, *et al*. Detection of wild-type EGFR amplification and EGFRvIII mutation in CSF-derived extracellular vesicles of glioblastoma patients. *Neuro Oncol. 2017*; 19(11):1494-1502.
44. Ge X, Pan MH, Wang L, Li W, Jiang C, He J, *et al*. Hypoxia-mediated mitochondria apoptosis inhibition induces temozolomide treatment resistance through miR-26a/Bad/Bax axis. *Cell Death Dis. 2018* Nov 13;9(11):1128.
45. Hajian-Tilaki K. Receiver Operating Characteristic (ROC) Curve Analysis for Medical Diagnostic Test Evaluation. *Caspian J Intern Med.2013*; 4(2):627-35.
46. Han S, Liu Y, Cai SJ, Qian M, Ding J, Larion M, *et al*. IDH mutation in glioma: molecular mechanisms and potential therapeutic targets. *Br J Cancer. 2020*; 122(11):1580-1589.
47. Horvitz H.R, Sulston J.E. Isolation and genetic characterization of cell-lineage mutants of the nematode Caenorhabditis elegans. *Genetics. 1980*; 96(2):435-54.
48. Ilyas M. Next-Generation Sequencing in Diagnostic Pathology. Pathobiology. 2017; 84(6):292-305.

49. Juratli TA, Stasik S, Zolal A, Schuster C, Richter S, Daubner D, *et al*. TERT Promoter Mutation Detection in Cell-Free Tumor-Derived DNA in Patients with IDH Wild-Type Glioblastomas: A Pilot Prospective Study. *Clin Cancer Res. 2018*; 24(21):5282-5291.
50. Khuong-Quang DA, Buczkowicz P, Rakopoulos P, Liu XY, Fontebasso AM, Bouffet E *et al.* K27M mutation in histone H3.3 defines clinically and biologically distinct subgroups of pediatric diffuse intrinsic pontine gliomas. *Acta Neuropathol. 2012*; 124:439-447.
51. Kui X, Wang Y, Zhang C, Li H, Li Q, Ke Y, Wang L. Prognostic value of SH3PXD2B (Tks4) in human hepatocellular carcinoma: a combined multi-omics and experimental study. *BMC Med Genomics. 2021*;14(1):115.
52. Lagos-Quintana M, Rauhut R, Lendeckel W, Tuschl T. Identification of novel genes coding for small expressed RNAs. *Science. 2001*; 294(5543):853-8.
53. Lawrie CH. MicroRNAs in hematological malignancies. *Blood Rev. 2013*; 27:143-154.
54. Lapointe S, Perry A, Butowski NA. Primary brain tumours in adults. *Lancet. 2018*; 392(10145):432-446.
55. Larrea E, Sole C, Manterola L, et al. New Concepts in Cancer Biomarkers: Circulating miRNAs in Liquid Biopsies. *Int J Mol Sci. 2016*; 17(5):627.
56. Lawrie CH, Gal S, Dunlop HM, Pushkaran B, Liggins AP, Pulford K, Banham AH, Pezzella F, *et al.* Detection of elevated levels of tumour-associated microRNAs in serum of patients with diffuse large B-cell lymphoma. *Br J Haematol. 2008*; 141(5):672-5.
57. Lee RC, Feinbaum RL, Ambros V.The C. elegans heterochronic gene lin-4 encodes small RNAs with antisense complementarity to lin-14. *Cell 1993*; 75(5):843-54.
58. Liu J, Huang Y, Cheng Q, Wang J, Zuo J, Liang Y, Yuan G. miR-1-3p suppresses the epithelial-mesenchymal transition property in renal cell cancer by downregulating Fibronectin 1. *Cancer Manag Res. 2019*; 11:5573-5587.
59. Li Y, Kowdley KV. Method for microRNA isolation from clinical serum samples. *Anal Biochem. 2012*; 431(1):69-75.
60. Liu X, Fortin K, Mourelatos Z. MicroRNAs: biogenesis and molecular functions. *Brain Pathol. 2008*; 18(1):113-21.
61. Liu Z, Jiang Z, Huang J, Huang S, Li Y, Yu S, *et al.* miR-7 inhibits glioblastoma growth by simultaneously interfering with the PI3K/ATK and Raf/MEK/ERK pathways. *Int J Oncol. 2014*; 44(5):1571-80.

62. Louis DN, Ohgaki H, Wiestler OD, Cavenee WK, Burger PC, Jouvet A, *et al*. The 2007 WHO classification of tumours of the central nervous system. *Acta Neuropathol. 2007*; 114(2):97-109.
63. Louis DN, Wesseling P, Aldape K, Brat DJ, Capper D, Cree IA *et al*. cIMPACT-NOW update 6: new entity and diagnostic principle recommendations of the cIMPACT-Utrecht meeting on future CNS tumor classification and grading. *Brain Pathol. 2020*; 30(4):844-856.
64. Martínez-Ricarte F, Mayor R, Martínez-Sáez E, Rubio-Pérez C, Pineda E, Cordero E, *et al.* Molecular Diagnosis of Diffuse Gliomas through Sequencing of Cell-Free Circulating Tumor DNA from Cerebrospinal Fluid. *Clin Cancer Res. 2018*; 24(12):2812-2819.
65. McFaline-Figueroa JR, Lee EQ. Brain Tumors. *Am J Med. 2018*; 131(8):874-882.
66. Metallo CM, Gameiro PA, Bell EL, Mattaini KR, Yang J, Hiller K, *et al*. Reductive glutamine metabolism by IDH1 mediates lipogenesis under hypoxia. *Nature. 2012;* 481(7381): 380-384.
67. Miao F, Cui C, Zuo D, Zhang H, Mei P, Chen H, *et al.* Rap2B promotes cell adhesion, proliferation, migration and invasion of human glioma. *J Neurooncol. 2019*;143:221-229.
68. Miller AM, Shah RH, Pentsova EI, Pourmaleki M, Briggs S, Distefano N, *et al*. Tracking tumour evolution in glioma through liquid biopsies of cerebrospinal fluid. *Nature. 2019;* 565(7741):654-658.
69. Mitchell PS, Parkin RK, Kroh EM, Fritz BR, Wyman SK, Pogosova-Agadjanyan EL *et al.* Circulating microRNAs as stable blood-based markers for cancer detection. *Proc Natl Acad Sci U S A. 2008*; 105: 10513-10518.
70. Molinari E, Curran OE, Grant R. Clinical importance of molecular markers of adult diffuse glioma. *Pract Neurol. 2019*; 19: 412-416.
71. Mondesir J, Willekens C, Touat M, de Botton S. IDH1 and IDH2 mutations as novel therapeutic targets: current perspectives. *J Blood Med. 2016;* 7:171-80.
72. Mo MH, Chen L, Fu Y, Wang W, Fu SW.Cell-free Circulating miRNA Biomarkers in. *J Cancer. 2012*; 3:432-48.
73. Müller Bark J, Kulasinghe A, Chua B, Day BW, Punyadeera C. Circulating biomarkers in patients with glioblastoma. *Br J Cancer. 2020*; 122: 295-305.
74. Nabavizadeh SA, Ware JB, Guiry S, Nasrallah MP, Mays JJ, Till JE *et al*. Imaging and histopathologic correlates of plasma cell-free DNA concentration and circulating tumor DNA in adult patients with newly diagnosed glioblastoma. *Neurooncol Adv.2020;* 2: vdaa016

75. Nayak L, Lee EQ, Wen PY. Epidemiology of brain metastases. *Curr Oncol Rep. 2012*; 14(1):48-54.
76. Nunez R. DNA measurement and cell cycle analysis by flow cytometry. *Curr Issues Mol Biol. 2001*;3(3):67-70.
77. Obuchowski NA, Bullen JA. Receiver operating characteristic (ROC) curves: review of methods with applications in diagnostic medicine. *Phys Med Biol. 2018*; 63(7):07TR01.
78. Orellana EA, Kasinski AL. MicroRNAs in Cancer: A Historical Perspective on the Path from Discovery to Therapy. *Cancers (Basel). 2015*; 7(3):1388-405.
79. Panditharatna E, Kilburn LB, Aboian MS, Kambhampati M, Gordish-Dressman H,Magge SN et al. Clinically Relevant and Minimally Invasive Tumor Surveillance of Pediatric Diffuse Midline Gliomas Using Patient-Derived Liquid Biopsy. *Clin Cancer Res. 2018*; 24: 5850-5859.
80. Parsons DW, Jones S, Zhang X, Lin JC, Leary RJ, Angenendt P, *et al*. An integrated genomic analysis of human glioblastoma multiforme. *Science. 2008*; 321(5897):1807-12.
81. Pisapia DJ. The Updated World Health Organization Glioma Classification: Cellular and Molecular Origins of Adult Infiltrating Gliomas. *Arch Pathol Lab Med. 2017*; 141(12):1633-1645.
82. Regazzo G, Terrenato I, Spagnuolo M, Carosi M, Cognetti G, Cicchillitti L *et al*. A restricted signature of serum miRNAs distinguishes glioblastoma from lower grade gliomas. *J Exp Clin Cancer Res. 2016*; 35(1):124.
83. Reinhart BJ, Weinstein EG, Rhoades MW, Bartel B, Bartel DP. MicroRNAs in plants. *Genes Dev. 2002*; 16(13):1616-26.
84. Reni M, Mazza E, Zanon S, Gatta G, Vecht CJ. Central nervous system gliomas. *Crit Rev Oncol Hematol. 2017*; 113:213-234.
85. Romanidou O, Kotoula V, Fountzilas G. Bridging Cancer Biology with the Clinic: Comprehending and Exploiting IDH Gene Mutations in Gliomas. Cancer Genomics *Proteomics. 2018*; 15(5):421-436.
86. Romero-Cordoba SL, Salido-Guadarrama I, Rodriguez-Dorantes M, Hidalgo-Miranda A. miRNA biogenesis: biological impact in the development of cancer. *Cancer Biol Ther. 2014*; 15(11):1444-55.
87. Rooj AK, Mineo M, Godlewski J. MicroRNA and extracellular vesicles in glioblastoma: small but powerful. *Brain Tumor Pathol. 2016*; 33(2):77-88.

88. Salkeni MA, Zarzour A, Ansay TY, McPherson CM, Warnick RE, Rixe O, Bahassi el M. Detection of EGFRvIII mutant DNA in the peripheral blood of brain tumor patients. *J Neurooncol. 2013*; 115(1):27-35.
89. Santangelo A, Tamanini A, Cabrini G, Dechecchi MC. Circulating microRNAs as emerging non-invasive biomarkers for gliomas. *Ann Transl Med. 2017*; 5(13):277.
90. Shaikh N, Dixit K, Raizer J. Recent advances in managing/understanding meningioma. *F1000Res. 201*8; 7. pii: F1000 Faculty Rev-490.
91. Shea A, Harish V, Afzal Z, Chijioke J, Kedir H, Dusmatova S, *et al.* MicroRNAs in glioblastoma multiforme pathogenesis and therapeutics. *Cancer Med. 2016*; 5(8):1917-46.
92. Siravegna G, Mussolin B, Venesio T, Marsoni S, Seoane J, Dive C, *et al*. How liquid biopsies can change clinical practice in oncology. *Ann Oncol. 2019*; 30(10):1580-1590.
93. Sohel MH. Extracellular/Circulating MicroRNAs: Release Mechanisms, Functions and Challenges. *Achievements in the Life Sciences.2016*; 10,175–186.
94. Thomas KT, Gross C, Gary J. Bassell microRNAs Sculpt Neuronal Communication in a Tight Balance That Is Lost in Neurological Disease Front. *Mol. Neurosci, 2018*.
95. Turkalp Z, Karamchandani J, Das S. IDH mutation in glioma: new insights and promises for the future. *JAMA Neurol. 2014*; 71(10):1319-25.
96. Turchinovich A, Weiz L, Langheinz A, Burwinkel B. Characterization of extracellular circulating microRNA. *Nucleic Acids Res. 2011*; 39(16):7223-33.
97. Valihrach L, Androvic P, Kubista M. Circulating miRNA analysis for cancer diagnostics and therapy. *Mol Aspects Med. 2020*; 72: 100825.
98. Vreugdenhil E, Berezikov E. Fine-tuning the brain: MicroRNAs. *Front Neuroendocrinol. 2010*; 31(2):128-33.
99. Visser M, Müller D.M.J, van Duijn R.J.M , Smits M, Verburg N, Hendriks E.J, Nabuurs R.J.A, *et al*. Inter-rater agreement in glioma segmentations on longitudinal MRI,*NeuroImage: Clinical,Volume 22, 2019.*
100. Wang J, Li X, Wu H, Wang H, Yao L, Deng Z, Zhou Y. EMP1 regulates cell proliferation, migration, and stemness in gliomas through PI3K-AKT signaling and CD44. *J Cell Biochem. 2019*;120:17142-17150
101. Wang S, Yin Y, Liu S. Roles of microRNAs during glioma tumorigenesis and progression. *Histol Histopathol. 2018*; 14:18040.

102. Wang Q, Li P, Li A, Jiang W, Wang H, Wang J, et al. Plasma specific miRNAs as predictive biomarkers for diagnosis and prognosis of glioma. *J Exp Clin Cancer Res. 2012*; 31:97.
103. Wang Z, Gerstein M, Snyder M. RNA-Seq: a revolutionary tool for transcriptomics. *Nat Rev Genet. 2009*; 10(1):57-63.
104. Wightman B, Ha I, Ruvkun G. Posttranscriptional regulation of the heterochronic gene lin-14 by lin-4 mediates temporal pattern formation in C. elegans. *Cell. 199*3; 75(5):855-62.
105. Williams Z, Ben-Dov IZ, Elias R, Mihailovic A, Brown M, Rosenwaks Z, Tuschl T. Comprehensive profiling of circulating microRNA via small RNA sequencing of cDNA libraries reveals biomarker potential and limitations. *Proc Natl Acad Sci U S A. 2013*; 12,110(11):4255-60.
106. Wolburg H, Wolburg-Buchholz K, Kraus J, Rascher-Eggstein G, Liebner S, Hamm S, *et al*. Localization of claudin-3 in tight junctions of the blood-brain barrier is selectively lost during experimental autoimmune encephalomyelitis and human glioblastoma multiforme. *Acta Neuropathol. 2003*; 105(6):586-92.
107. Wolburg H, Noell S, Fallier-Becker P, Mack A.F, Wolburg-Buchholz K, The disturbed blood–brain barrier in human glioblastoma, Molecular *Aspects of Medicine.2012*;33(5-6)579-589.
108. Xu K, Qiu C, Pei H, Mehmood MA, Wang H, Li L, Xia Q. Homeobox B3 promotes tumor cell proliferation and invasion in glioblastoma. *Oncol Lett. 2018*;15:3712-3718.
109. Yang C, Wang C, Chen X, Chen S, Zhang Y, Zhi F, *et al*. Identification of seven serum microRNAs from a genome-wide serum microRNA expression profile as potential noninvasive biomarkers for malignant astrocytomas. *Int J Cancer. 2013*; 132(1):116-27.
110. Yang Y, Wang J, Xu S, Lv W, Shi F, Shan A. IKBIP is a novel EMT-related biomarker and predicts poor survival in glioma. *Transl Neurosci. 2021*;12:9-19.
111. Zhi F, Shao N, Wang R, Deng D, Xue L, Wang Q, *et al.* Identification of 9 serum microRNAs as potential noninvasive biomarkers of human astrocytoma. *Neuro Oncol.2015*; 17: 383-391.
112. Zhang H, Kolb FA, Jaskiewicz L, Westhof E, FilipowiczW. Single processing center models for human Dicer and bacterial RNase III. *Cell. 2004*; 118(1):57-68.
113. Zhang H, Wang J, Wang Z, Ruan C, Wang L, Guo H. Serum miR-100 is a potential biomarker for detection and outcome prediction of glioblastoma patients. *Cancer Biomark. 2019*; 24: 43-49.

114. Zhang L, He L, Lugano R, Roodakker K, Bergqvist M, Smits A, Dimberg A. IDH mutation status is associated with distinct vascular gene expression signatures in lower-grade gliomas. *Neuro Oncol. 2018*;20:1505-1516.
115. Zhang Y, Ta WW, Sun PF, Meng YF, Zhao CZ. Diagnostic and prognostic significance of serum miR-145-5p expression in glioblastoma. *Int J Clin Exp Pathol.2019*; 12: 2536-2543.
116. Zhong F, Huang T, Leng J. Serum miR-29b as a novel biomarker for glioblastoma diagnosis and prognosis. *Int J Clin Exp Pathol. 2019*; 12: 4106-4112.
117. Zhou Q, Liu J, Quan J, Liu W, Tan H, Li W. MicroRNAs as potential biomarkers for the diagnosis of glioma: A systematic review and meta-analysis. *Cancer Sci. 2018*; 109(9):2651-2659.

Rome, 20th July 2021

Ana Belén Díaz Méndez

Dept. of Research, Advanced Diagnostics and
Technological Innovation.
Oncogenomic and Epigenetic Unit- Translational Research Area
Regina Elena National Cancer Institute, Rome, Italy.
E-mail:anabelen.diaz@ifo.gov.it

Tutor: Maria Giulia Rizzo, PhD

Dept. of Research, Advanced Diagnostics and
Technological Innovation.
Oncogenomic and Epigenetic Unit- Translational Research Area
Regina Elena National Cancer Institute, Rome, Italy.
E-mail:maria.rizzo@ifo.gov.it
Phone number: 39 - 6 -5266-2522